Precambrian Research 224 (2013) 222–241

Contents lists available at SciVerse ScienceDirect

Precambrian Research

journal homepage: www.elsevier.com/locate/precamres

Proterozoic evolution of the Mojave crustal province as preserved in the Ivanpah Mountains, southeastern California

By Ariel Strickland[a,d,*], Joseph L. Wooden[a,b], Chris G. Mattinson[a,c], Takayuki Ushikubo[d], David M. Miller[b], John W. Valley[d]

[a] Department of Geological and Environmental Sciences, Stanford University, Stanford, CA 94305, United States
[b] U.S. Geological Survey, Menlo Park, CA 94025, United States
[c] Department of Geological Sciences, Central Washington University, Ellensburg, WA 98926, United States
[d] Department of Geosciences, University of Wisconsin, Madison, WI 53706, United States

ARTICLE INFO

Article history:
Received 6 March 2012
Received in revised form 1 September 2012
Accepted 4 September 2012
Available online 14 September 2012

Keywords:
Mojave province
Proterozoic
Zircon
Monazite
Migmatites
1.67 Ga extension

ABSTRACT

In the western U.S., numerous exposures of Precambrian crustal rocks were exhumed from mid-crustal depths during Cenozoic tectonic events and provide a view into the deep crust. This natural laboratory provides an excellent opportunity to study orogenic and continent-forming processes at deeper levels. The Ivanpah Mountains of southeastern California contain exposures of Paleoproterozoic migmatites and banded gneisses that belong to the Mojave crustal province. New, detailed U–Pb geochronology of monazite and zircon from ortho- and paragneisses reveal the timing of the formation of these rocks and multiple periods of metamorphism and magmatism. Paragneisses have detrital zircon populations of dominantly 1.80–2.15 Ga (dominant) and 2.4–2.8 Ga, although the youngest detrital zircon grain is 1.754 ± 24 Ga. Values of δ^{18}O(zircon) of the two detrital age populations are 7.0 ± 2.2‰ and 6.3 ± 1.4‰ (2SD), respectively, consistent with original, igneous values. Based on the 1.76 Ga age of metamorphic zircon rims, the metasediments were intruded by a calc-alkaline magmatic suite including gabbro, tonalite, and porphyritic granite at 1.76 Ga, although the contacts are obscured by pervasive metamorphism and deformation.

U–Pb ages of metamorphic overgrowths on detrital zircons from the paragneisses indicate multiple events at ~1.76, 1.74, 1.70 and 1.67 Ga which documents a periodicity of tectonism through time. The oxygen isotope ratios of the metamorphic zircon overgrowths from the paragneisses remained relatively constant through time within each sample, consistent with growth during in situ partial melting. However, oxygen isotope ratios of zircons from 1.74 Ga leucocratic material are lower in δ^{18}O, and therefore could not have been generated by partial melting of the adjacent paragneiss. Monazite from both igneous and metasedimentary rocks preserves two periods of growth at 1.75 and 1.67 Ga. In situ, U–Pb dating of monazite reveals that 1.67 Ga monazite inclusions are found in major rock-forming minerals, and therefore we interpret this as the timing of fabric formation and migmitization, which is younger than previously believed and is interpreted to be the dominant metamorphic pulse in the protracted middle crustal tectonism. Thermobarometry indicates peak metamorphic conditions of ~3.5 kb and ~740 °C, which is consistent with partial melting and the metamorphic mineral assemblage in these rocks (sillimanite + K-feldspar, muscovite absent). This paper shows (1) multiple pulses identified within 100 Ma orogeny, (2) zircon components and their overgrowths demonstrate mixing of Archean, 1.8 and younger reservoirs, (3) low pressure granulite facies metamorphism occurred at 1.67 Ga and may have been related to continental extension of a tectonically over-thickened crust.

1. Introduction

Exposures of deeply exhumed rocks can provide an understanding of the formation of continents and the growth of cratons through periods of accretion. In the western United States, widespread exposures of Precambrian crust have been exhumed by Mesozoic and Cenozoic tectonic events. The signature of the processes that assemble continents is recorded in these complex middle crustal exposures that have undergone protracted or multiple events.

Distinct Proterozoic crustal provinces have been identified (e.g., Condie, 1982; Bennett and DePaolo, 1987; Wooden and DeWitt,

* Corresponding author.
E-mail address: strick@geology.wisc.edu (B.A. Strickland).

0301-9268/$ – see front matter © 2012 Elsevier B.V. All rights reserved.
http://dx.doi.org/10.1016/j.precamres.2012.09.006

1991), although the order and timing of assembly of these provinces is still debated (e.g. Duebendorfer et al., 2006; Whitmeyer and Karlstrom, 2007; Amato et al., 2008). This paper shows how a detailed tectonic history can be unraveled in a key type-area using zircon and monazite geochronology, thermobarometry and stable isotope geochemistry.

From about 1.8 to 1.6 Ga, newly formed continental crust was added to southern Laurentia during a significant period of crustal growth (e.g., Condie, 1982; Karlstrom and Bowring, 1988; Hoffman, 1988; Karlstrom et al., 2001). Paleoproterozoic crust of this age forms approximately 20% of the North American craton and stretches from southern California to Nova Scotia along a NE trend (for details see Whitmeyer and Karlstrom, 2007). Geochronologic, isotopic, and structural studies have defined crustal provinces and terranes that generally young to the south/southeast with increasing distance from the Archean craton (e.g. Condie, 1982; Bennett and DePaolo, 1987; Karlstrom and Bowring, 1988; Amato et al., 2008). Much of this crust has been interpreted as juvenile island arcs and marginal basins that formed with limited involvement of pre-existing continental crust (e.g., Condie, 1982; Bennett and DePaolo, 1987; Karlstrom and Bowring, 1988; Wooden and DeWitt, 1991). However, Shufeldt et al. (2010) documented Archean and 1.8–2.0 Ga detritus in the Vishnu schist of Grand canyon, which implies that this sequence was derived, at least in part, from older crust.

The Mojave crustal province of western Arizona and southeastern California (Fig. 1) is distinct from the other Paleoproterozoic crustal provinces based and Nd and Pb isotopic studies (e.g., Bennett and DePaolo, 1987; Wooden and DeWitt, 1991; Duebendorfer et al., 2006). The Mojave province was originally defined by rocks with Nd model ages of 2.0–2.3 Ga, which is significantly older than their crystallization ages (Bennett and DePaolo, 1987). Studies of Pb isotopic compositions have shown that the Mojave crust is significantly more radiogenic when compared to the relatively juvenile Pb isotopic compositions of the adjacent Yavapai province, and that the Mojave crust has an inherently higher Th/U ratio (Wooden and Miller, 1990; Wooden and DeWitt, 1991; Barth et al., 2000; Duebendorfer et al., 2006). SHRIMP U–Pb ages of detrital zircons from Paleoproterozoic metasediments in the Mojave province have documented abundant Archean detrital zircons and inherited Archean zircons have been reported in plutonic samples from the Mojave province (Barth et al., 2000; Bryant et al., 2001; Strickland et al., 2009; Shufeldt et al., 2010). Therefore, the Mojave province, unlike other Paleoproterozoic crust such as the adjacent Yavapai province, likely incorporated a significant amount of older, pre-existing crustal material during its formation ca. 1.79–1.74 Ga (Bennett and DePaolo, 1987; Wooden and Miller, 1990; Barth et al., 2000; Duebendorfer et al., 2010).

The Ivanpah Mountains of southeastern California (Fig. 1) contain a relatively unstudied Proterozoic migmatite terrane that belongs to the Mojave crustal province. The purpose of this paper is to characterize the Paleoproterozoic rocks exposed in the Ivanpah Mountains and to determine the timing and nature of tectonic events that they preserve. Detailed U–Pb geochronology of zircon and monazite, and zircon oxygen isotope ratios measured by secondary ionization mass spectrometery (SIMS) combined with thermobarometry and field relations are combined to identify potentially four periods of metamorphism and/or magmatism between 1.76 and 1.67 Ga. The goals of this paper are (1) to establish the ages preserved in the rocks of the Ivanpah Mountains and try to relate them to fabrics and tectonic events, (2) to compare and contrast zircon and monazite formation in multiply-metamorphosed rocks, (3) to use oxygen isotopes to determine the nature of zircon growth, (4) to use in situ analytical techniques to determine the formation of the penetrative migmatitic fabric, and (5) to use thermobarometry to determine the pressure and temperature of the migmatization. This study will provide a detailed fingerprint of the crust of the Mojave province that is necessary for paleocontinent reconstructions, and will help to constrain the growth of continental crust along the southern margin of Laurentia during the Paleoproterozoic. We demonstrate that the timing of migmatite formation in the Ivanpah Mountains was likely ca. 1.67 Ga, and may have occurred in an extensional setting.

2. Geologic setting

Exposures of Paleoproterozoic basement in the southwestern United States preserve a record of crust formation and amalgamation along a long-lived convergent margin (e.g., Karlstrom and Bowring, 1988). In the Mojave province, the oldest known rock is the 1.84 Ga Elves Chasm tonalite gneiss (Hawkins et al., 1996; Ilg et al., 1996), but due to the limited exposure in the Granite Gorge of the Grand Canyon its tectonic significance is unclear. Whitmeyer and Karlstrom (2007) interpreted the Elves Chasm gneiss to be part of a 2.0–1.8 Ga juvenile arc that was juxtaposed with an Archean (Mojave) block and tectonic mixing of these blocks. The oldest rocks that are regionally exposed in the Mojave province are metasedimentary gneisses (Thomas et al., 1988; Wooden and Miller, 1990) that were deposited ~1.79–1.75 Ga based on detrital zircon studies (Barth et al., 2000, 2009; this study). The metasedimentary rocks in the San Bernardino Mountains (Fig. 1) contain detrital zircons with a characteristic suite of ages that fall into two populations: 1.8–2.1 Ga (dominant) and 2.4–2.9 Ga (Barth et al., 2009), which is very similar to the detrital zircons in the Vishnu Schist of Grand Canyon (Shufeldt et al., 2010).

A 1.79–1.76 Ga, pre-orogenic magmatic suite that includes gabbro, tonalite, trondhjemite and porphyritic granite is also widespread throughout the Mojave province (Thomas et al., 1988; Wooden and Miller, 1990; Barth et al., 2000). This early magmatism has a calc-alkalic affinity and has been interpreted as arc-related (e.g. Wooden and Miller, 1990; Ilg et al., 1996; Barth et al., 2000, 2009; Duebendorfer et al., 2001, 2010). These protoliths are highly deformed and metamorphosed from upper amphibolite facies to lower granulite facies (Thomas et al., 1988; Young, 1989; Wooden and Miller, 1990).

A phase of regional metamorphism in the Mojave province occurred ca. 1.74 Ga (Barth et al., 2000, 2009; Duebendorfer et al., 2001). In the Cerbat Mountains of western Arizona (Fig. 1), Duebendorfer et al. (2001) describe an early N/NW-striking fabric that formed during metamorphic conditions of 675 to ~740 °C and 5–6 kb. Cross-cutting relations and U–Pb zircon ages of plutonic rocks from the Cerbat Mountains bracket this period of deformation to 1.74–1.72 Ga. In the San Bernardino Mountains of southern California (Fig. 1), Barth et al. (2000) reported low Th/U overgrowths on detrital zircons that indicate a metamorphic event occurred at ~1.74 Ga. Magmatism of this age is common in the Yavapai province (Karlstrom and Bowring, 1988), suggesting that the two terranes may have been juxtaposed at or before 1.74 Ga (Barth et al., 2000; Duebendorfer et al., 2001; Whitmeyer and Karlstrom, 2007).

Another major period of deformation occurred between 1.71 and 1.69 Ga in both the Mojave and adjacent Yavapai provinces (Wooden and Miller, 1990; Barth et al., 2000, 2009; Bryant et al., 2001; Duebendorfer et al., 2001). Wooden and Miller (1990) termed this event the Ivanpah orogeny because the best examples of deformation of this age are found in the mountain ranges surrounding the Ivanpah Valley, and this orogeny may be correlative to the Yavapai orogeny in Arizona (Whitmeyer and Karlstrom, 2007). Early plutonic and supracrustal rocks were strongly deformed and metamorphosed to upper amphibolite–lower granulite facies between ~1.71 and 1.69 Ga based on the ages of pre-, syn-, and post-tectonic

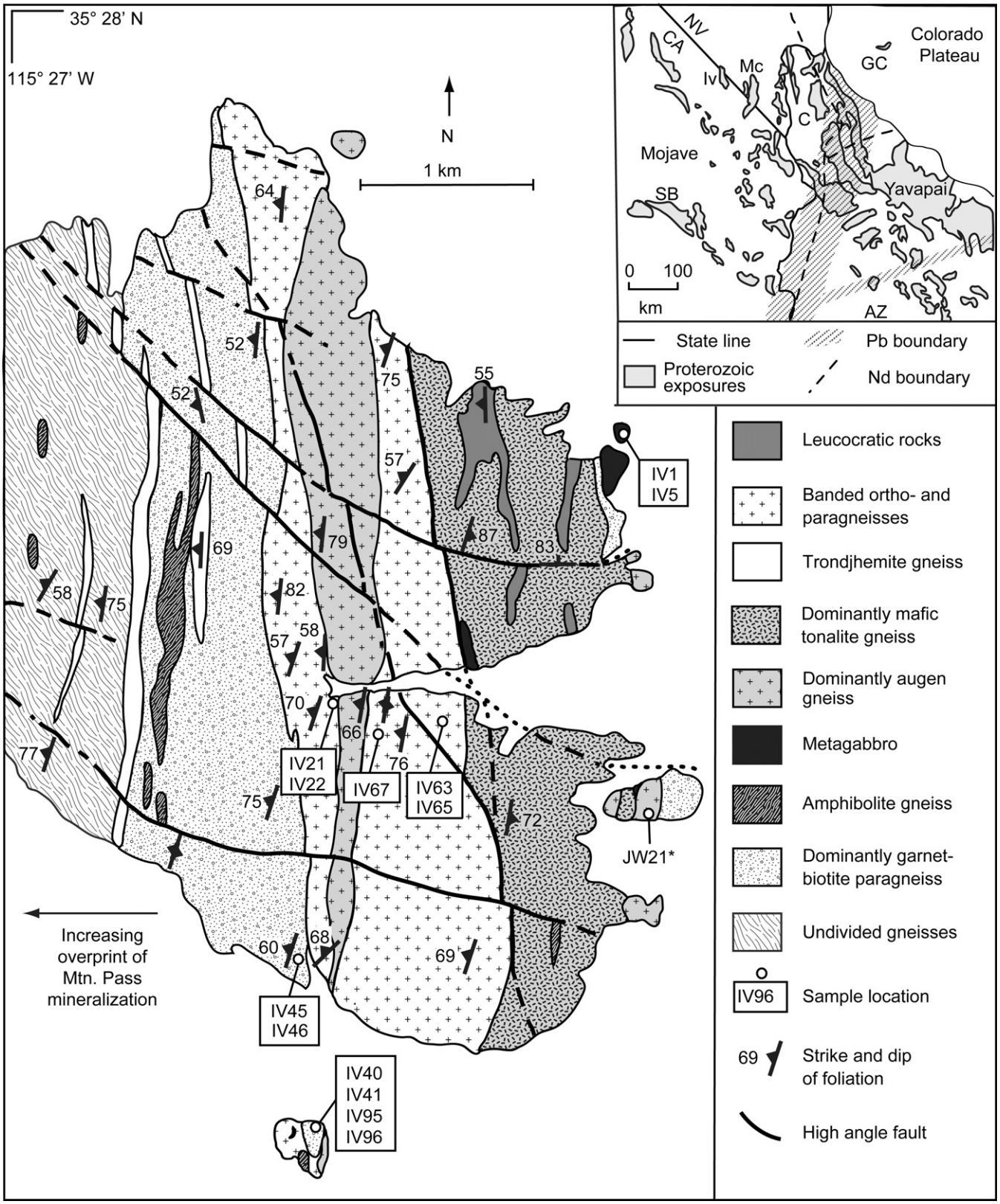

Fig. 1. Generalized geologic map of the Proterozoic rocks in the Ivanpah Mountains based on Miller and Wooden (1994). The banded gneisses are lithologically heterogeneous and the map units are based on the dominant lithology. Undivided gneisses in the western part of the map area have been altered and mineralized. Sample locations from this study are shown in addition to JW21* which is from Barth et al. (2009). Inset at upper right shows the location of the Ivanpah Mountains (Iv), the San Bernardino Mountains (SB), the McCullough Mountains (Mc), the Cerbat Mountains (C), and the Grand Canyon (GC).

plutons (Wooden and Miller, 1990; Karlstrom and Williams, 1995; Hawkins et al., 1996; Duebendorfer et al., 2001). In the Upper Granite Gorge of Grand Canyon, Hawkins et al. (1996) identified metamorphic monazite growth from 1.706 to 1.697 Ga, and correlated it to lower granulite facies metamorphism. In the Cerbat Mountains of western Arizona (Fig. 1), Duebendorfer et al. (2001) describe a penetrative, NE-striking fabric (their D_2) that developed at 650–700 °C and 3.5–4.5 kb. The timing of this event is bracketed in the Cerbat Mountains by the ages of pre- and post-orogenic granites to 1721–1682 (Duebendorfer et al., 2001). The NE-striking, steeply dipping fabric described in the Cerbat Mountains is the dominant fabric found across the Yavapai province (Karlstrom and Bowring, 1988; Karlstrom and Humphreys, 1998). Barth et al. (2000) proposed that The Ivanpah orogeny was related to the collision of the Mojave and Yavapai provinces, whereas Duebendorfer et al. (2001) proposed that the 1.70 Ga event recorded the collision of the combined Mojave and Yavapai provinces with North America. Whitmeyer and Karlstrom (2007) simply used the term Yavapai orogeny for the protracted event from 1.78 to 1.68 Ga that affected SW Laurentia.

Post-orogenic, 1.69–1.65 Ga granitic plutons and pegmatites are widespread across the Mojave province and reflect a fundamental change from early calc-alkaline magmatism with an arc affinity to more potassic, A-type, granitic melts (Wooden and Miller, 1990; Barth et al., 2009). This suite of igneous rocks is typically undeformed and crosscuts structural trends, however, in the San Bernardino Mountains (Fig. 1), plutons as young as 1.675 Ga are deformed (Barth et al., 2000). In the New York/McCullough Mountains (Fig. 1), plutons ranging from 1.695 to 1.659 Ga form a batholith-sized igneous complex (Wooden and Miller, 1990). In the Granite Gorge of Grand Canyon, post-orogenic granites and pegmatites form up to 50% of the exposures (Hawkins et al., 1996; Ilg et al., 1996). Thus, major change from early calc-alkaline magmatism to evolved granitic magmatism may represent the final phase of crust formation and stabilization in the Mojave province.

3. The Ivanpah Mountains

The Ivanpah Mountains are located in the central Mojave province more than 100 km to the west of the isotopically mixed boundary with the Yavapai province, and can be viewed as a type-location for Mojave crust (Wooden and Miller, 1990; Duebendorfer et al., 2006). In the eastern Ivanpah Mountains of southeastern California (Fig. 1), exposures of Proterozoic crystalline basement are characterized by series of banded gneisses of both igneous and sedimentary origin. These rocks were transposed into a migmatitic layering on all scales such that primary sedimentary features have been erased and protoliths are often difficult to determine in the field. In this study, rocks were determined to be metasedimentary or metaigneous based on the zircon results. The lithologic units shown on Fig. 1 represent the dominant lithologies within each area. The migmatitic layering and penetrative foliation are N/S-striking and subvertical or steeply dipping to the west (Fig. 1). Mineral elongation lineations are rare, but typically steep. In the western portion of the mapped area in Fig. 1, the Paleoproterozoic migmatites are overprinted by alteration and mineralization related to the intrusion of the 1.4 Ga Mountain Pass carbonatite complex which lies ~10 km to the northwest of the area in Fig. 1 (DeWitt et al., 1987).

The paragneisses are likely the oldest rocks exposed in the Ivanpah Mountains (Fig. 1) (Wooden and Miller, 1990; this study). Paragneisses are dominantly metagreywacke garnet–biotite gneiss with minor amounts of amphibolite, pelite and quartzite, and abundant leucosomal segregations (Fig. 2; Wooden and Miller, 1990). The rocks herein referred to as

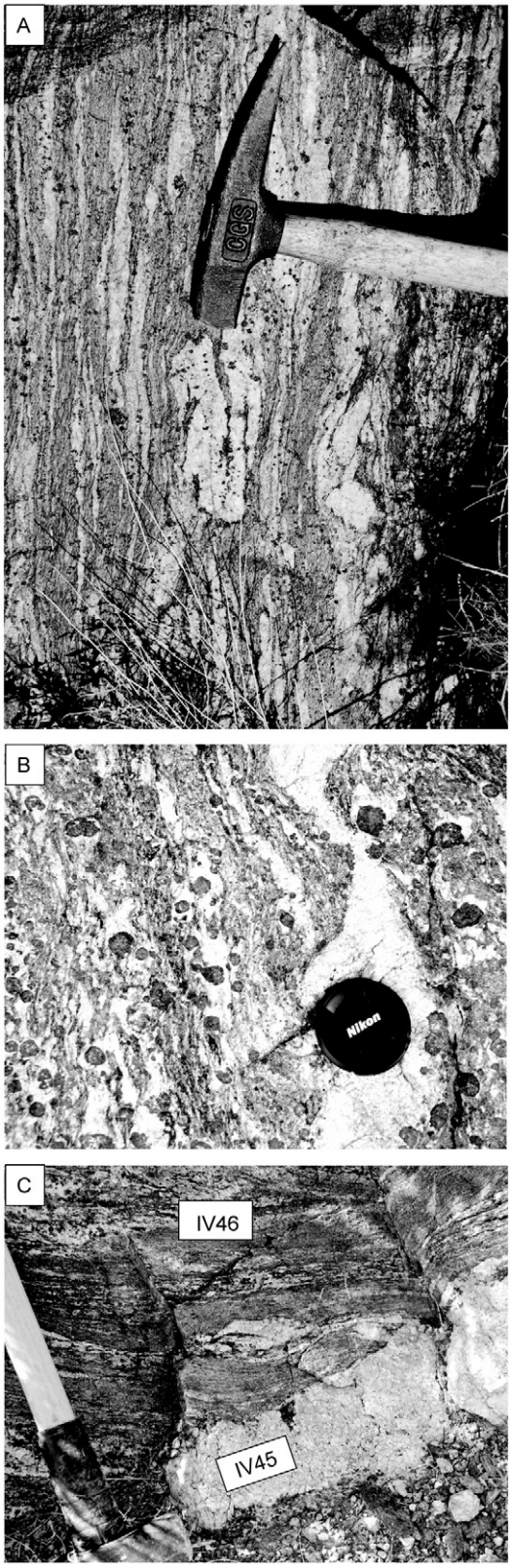

Fig. 2. Migmatites of the Ivanpah Mountains. Top: garnet–biotite gneiss with finely layered and folded leucosomal segregations. Hammer for scale. Center: Garnet–biotite with large garnets, many >3 cm in diameter. Lens cap for scale is 7 cm in diameter. Bottom: garnet–biotite gneiss (sample IV46) and leucocratic dike (sample IV45). The migmatitc layering in the garnet–biotite gneiss is crosscut by the dike. Hammer for scale.

garnet–biotite gneiss contain the peak metamorphic assemblage of garnet + biotite + quartz + plagioclase + K-feldspar + sillimanite (fibrolite), and cordierite, with up to 70% garnet, and with garnet sizes of up to 10 cm. These garnet–biotite gneisses are geochemically similar to immature clastic or volcanoclastic sediments (Wooden and Miller, 1990). Although nearly all the rocks contain a penetrative, N/S-striking, steeply dipping foliation, the metamorphic minerals in the garnet–biotite gneiss are typically medium to coarse grained with a granoblastic texture, indicating that high temperature metamorphic conditions outlasted or kept pace with ductile deformation, and that the final phase of metamorphism obliterated all pre-existing textures (Wooden and Miller, 1990).

In the eastern half of the field area (Fig. 1), exposures are largely comprised of an igneous suite of metatonalite, augen gneiss, and metagranite, with minor amounts of coarse grained, plagioclase-rich metagabbro and fine-grained amphibolite gneiss. Wooden and Miller (1990) reported a U–Pb zircon age of 1760 ± 20 for a metatonalite from the eastern Ivanpah Mountains. In addition, Barth et al. (2009) reported a U–Pb zircon age of 1.766 Ga for the augen gneiss exposed in the eastern Ivanpah Mountains (labeled "JW21" on Fig. 1). Although contacts are obscured by penetrative deformation and high-grade metamorphism, Wooden and Miller (1990) interpreted that the 1.76 Ga magmatic suite intruded the metasediments in the Ivanpah Mountains.

Leucocratic rocks, granites and pegmatites occur in many forms. In metaigneous rocks such as tonalite or augen gneiss, cm-scale leucocratic layering is common and may reflect intrusion of leucocratic dikes and veins rather than in situ partial melting. In the paragneisses, leucosomes occur as fine-scale segregations that are interfingered with the host gneiss and appear to coalesce into larger melt pockets, indicative of partial melting (Fig. 2). Most leucocratic segregations are highly deformed (Fig. 2). Leucocratic layering of dikes and sills often define the migmatitic layering. N/S-striking, seemingly undeformed, garnet-bearing leucocratic dikes crosscut all lithologies at low angles to foliation (Fig. 2). Field relations show that both partial melting of the paragneisses and intrusion of evolved magmas may have occurred simultaneously.

4. Methods

Samples collected from the Ivanpah Mountains were chosen to reflect a variety of rock types and degrees of deformation for the purpose of identifying multiple periods of deformation and metamorphism. U–Pb ages of zircon and monazite were determined using the U.S.G.S./Stanford University SHRIMP-RG in multiple sessions. Data reduction follows the methods described by Williams (1997) and Ireland and Williams (2003) and uses the Squid and Isoplot programs of Ken Ludwig. For all zircon samples, concordia intercept ages are preferred. Lower intercepts typically do not intercept zero, but instead yield Mesozoic ages as is typical for samples from the Mojave Province (e.g., Wooden and Miller, 1990; Barth et al., 2009). Discussions of individual detrital zircon grain ages use ^{204}Pb-corrected ^{207}Pb/^{206}Pb ages. For monazites, ages were calculated from uncorrected data (see Appendix A for details). Geochronologic data are summarized in Tables 1 and 2. Additional details of the analytical technique are provided in Appendix A. Data for zircon geochronology are provided in Appendix 2, and monazite geochronologic data are provided in Appendix 3. All errors are given as two sigma uncertainty.

Electron microprobe analysis by wavelength dispersive spectrometry was performed with the 5 spectrometer Cameca SX51 electron probe in the Geoscience Department of the University of Wisconsin-Madison. Samples and standards were coated with ~200 Å carbon. Operating conditions for analysis were 15 kV accelerating voltage with a beam current of 30 nA (Faraday cup) and a beam focused at 1 μm, creating an excitation area 3 μm in diameter. Automation and matrix corrections were performed with Probe for EPMA software (Armstrong, 1995; Donovan et al., 2010). See Appendix 4.

Oxygen isotope ratios in the same zircons that were dated by SHRIMP-RG were measured with a CAMECA IMS-1280 at the University of Wisconsin using the conditions and protocols outlined in Kita et al. (2009) and Valley and Kita (2009). The oxygen isotope ratios reported below were calculated using standard δ notation in per mil relative to the Vienna Standard of Mean Ocean Water, VSMOW. After analysis, the oxygen isotope pits were imaged by SEM, and pits that were accidentally placed on inclusions or cracks are excluded from the results. See Appendix A for details of the method and see Appendix 5 for oxygen isotope data.

5. Igneous rocks

5.1. Metagabbro

Samples IV1 and IV5 are from metagabbro exposed in the eastern Ivanpah Mountains (Fig. 1; Table 1). The metagabbro is coarse grained, granoblastic to porphyritic with large plagioclase crystals in a matrix of equigranular clinopyroxene and orthopyroxene. Cathodoluminescence images of zircons from the metagabbro show irregular, embayed grains with oscillatory zonation and thin, low-U overgrowths (Fig. 3). Analyses of the zircon interiors from the two samples produced concordia intercept ages of 1764 ± 12 and 1759 ± 8 Ma (Fig. 4). Analyses of the narrow, low-U zircon overgrowths from the metagabbro samples gave concordia ages of 1671 ± 17 and 1645 ± 33 Ma (Fig. 4). The low precision on the overgrowths is due to the low-U concentrations (<70 ppm, Appendix 2). As igneous zircon is rare in gabbro, it is possible that both core and overgrowth are metamorphic.

5.2. Leucocratic rocks

Leucocratic rocks are widespread in the Ivanpah Mountains, including deformed leucocratic segregations, deformed leucocratic layering on the centimeter to meter scale, and late, cross-cutting leucocratic, garnet-bearing dikes (Fig. 2). Due to the penetrative nature of the deformation, it is difficult to discern the origin of the deformed leucocratic rocks (e.g., in situ partial melting vs. injection). Samples of deformed and undeformed leucocratic material were chosen to bracket the timing of deformation.

Sample IV21 is from a folded, garnet and biotite-bearing pegmatite that intruded a granitic gneiss. Zircons from sample IV21 are complex and have irregular, oscillatory zoned cores with dark, weakly-zoned overgrowths (Fig. 3). Thirty-five analyses of zircon from the pegmatite reveal a spread of ^{207}Pb/^{206}Pb ages from 1636 ± 18 to 1757 ± 16 Ma that are concordant or nearly concordant (Fig. 5). Analyses from the irregular, oscillatory zoned cores yield a concordia intercept age of 1744 ± 10 Ma (Fig. 5). This age is interpreted as the crystallization age for the pegmatite. This early generation of zircons in the pegmatite closely post-dates the 1760 Ma metamorphic grains in the metagabbro and implies flux of lower crustal melts at this time. CL-dark overgrowths on zircons from sample IV21 form two populations on concordia (Fig. 5). Ten analyses of zircon overgrowths have an age of 1656 ± 9 Ma. These analyses represent zircons with fairly low ^{232}Th/^{238}U ratios (0.08–0.31) which are consistent with metamorphic growth. Finally, a subset of six analyses of unzoned overgrowths yields a concordia intercept age of 1708 ± 12 Ma. These rim ages likely indicate later metamorphism that affected this pegmatite.

Sample IV40 is a leucosomal layer approx 20 cm thick that is complexly folded with the adjacent garnet–biotite gneiss

Table 1
Summary of igneous samples, location, U–Pb geochronology and zircon oxygen isotope ratios.

Sample name	Lat/Long/Elevation	Lithology	Mineral assemblage	Strike and dip	Igneous zircon ages (Ma)	Metamorphic zircon ages (Ma)	Monazite U–Pb age (Ma)	δ^{18}O VSMOW zircon with 2SD‰	δ^{18}O VSMOW ‰ garnet (laser fluorination)
IV1	N35°26.577′, W115°24.835′, 913 m	Metagabbro	Plagioclase, clinopyroxene, orthopyroxene, hornblende, minor carbonate and talc	–	1764 ± 12, MSWD = 1.6	U-poor rims: 1671 ± 17, MSWD = 0.82	–	–	–
IV5	N35°26.577′, W115°24.835′, 913 m	Metagabbro	Plagioclase, clinopyroxene, orthopyroxene, hornblende, minor carbonate and talc	–	1759 ± 8, MSWD = 0.88	U-poor rims 1645 ± 33, MSWD = 0.87	–	–	–
IV21	N35°25.771′, W115°25.849′, 1077 m	Folded pegmatite	Quartz, K-feldspar, plagioclase, biotite, garnet	Fold hinge plunges 12° towards 0 1 0	1744 ± 10, MSWD = 0.94	1708 ± 12, MSWD = 0.39 and 1655 ± 9, MSWD = 1.2	–	6.4 ± 1.2 (n = 7), 6.7 ± 0.9 (n = 5) and 7.0 ± 2.1 (n = 3)	6.62
IV40	N35°24.429′, W115°26.003′, 1114 m	Deformed leucosome	Quartz, K-feldspar, plagioclase, biotite, minor garnet	1 7 0; 70W no lineation	1737 ± 18, MSWD = 22	–	1656 ± 5, MSWD = 1.8	4.3 ± 0.6 (n = 8)	6.98
IV45	N35°24.980′, W115°26.056′, 1137 m	Leococratic dike	Quartz, plagioclase, garnet, K-feldspar	1 6 3; 77W no lineation	1663 ± 6, MSWD = 1.2	–	1660 ± 3, MSWD = 1.4	9.9 ± 0.3 (n = 14)	9.02
IV95	N35°24.257, W115°26.02, 1108 m	Leococratic dike	Quartz, plagioclase, biotite	0 0 5; 75W no lineation	1730 ± 25, MSWD = 19	–	–	–	–
IV96	N35°24.259, W115°2603, 1111 m	Leococratic dike	Quartz, plagioclase, garnet, K-feldspar	0 1 0; 83W no lineation	1661 ± 9, MSWD = 2.3	–	–	6.9 ± 0.3 (n = 12)	6.93

Table 2
Summary of metasedimentary samples, location, U–Pb geochronology and zircon oxygen isotope ratios.

Sample name	Lat/Long/ Elevation	Lithology	Mineral assemblage	Strike and dip	Igneous zircon ages (Ma)	Metamorphic zircon ages (Ma)	Monazite U–Pb age (Ma) cores	Monazite U–Pb age (Ma) rims	δ^{18}O VSMOW zircon rims with 2SD‰ (SIMS)	δ^{18}O VSMOW garnet (laser fluorination)
IV22	N35°25.769′, W115°25.672′, 1057 m	Meta quartzite	Quartz, biotite, garnet	0 1 0; 75E, 60° towards 0 3 0	1764–2776. $N = 29$	1760 ± 18, MSWD = 1.6	1665 ± 12, MSWD = 2.8	1739 ± 10, MSWD = 0.9	9.0 ± 0.5 ($n = 4$) and 6.3 ± 0.8 ($n = 4$)	9.06
IV41	N35°24.429′, W115°26.003′, 1113 m	Garnet–biotite gneiss	Garnet, biotite, plagioclase, K-feldspar, quartz, cordierite, sillimanite	0 1 0; 60W 50° towards 3 2 0 but lineation weak	1779–2847. $N = 16$	1658–1773. $N = 28$	1676 ± 9, MSWD + 1.1	1748 ± 3, MSWD = 1.2	6.8 ± 1 ($n = 8$)	6.79
IV46	N35°24.980′, W115°26.056′, 1137 m	Garnet–biotite gneiss	Garnet, biotite, plagioclase, K-feldspar, cordierite, sillimanite	0 0 4; 74W, 34° towards 0 0 3	1754–2873. $N = 55$	1702 ± 7, MSWD = 0.77	1674 ± 4, MSWD = 0.54	1748 ± 4, MSWD = 3.5	10.5 ± 0.4 ($n = 9$)	9.97
IV63	N35°25.387′, W115°24.879′, 976 m	Garnet–biotite gneiss	Garnet, quartz, biotite, microcline, plagioclase, sillimanite	–	1792–2699. $N = 49$	1647–1765. $N = 26$	1668 ± 3, MSWD = 1.5	1742 ± 2, MSWD = 1	9.2 ± 1.8 ($n = 12$)	8.82
IV65	N35°25.484′, W115°25.447′, 1087 m	Garnet–biotite gneiss	Garnet, biotite, quartz, microcline, plagioclase, sillimanite, cordierite, spinel, muscovite	–	1766–2705. $N = 6$	1661 ± 12, MSWD = 0.45	1680 ± 3, MSWD = 1.1	1745 ± 9, MSWD = 1.2	–	7.69
IV67	N35°25.473′, W115°25.522′, 1099 m	Garnet–biotite gneiss	Garnet, biotite, quartz, microcline, plagioclase, cordierite, sillimanite, spinel	–	1754–2991. $N = 29$	1738 ± 20, MSWD = 3.9 and 1659 ± 23, MSWD = 2.1	–	–	9.3 ± 1.2 ($n = 13$) and 7.7 ± 0.5 ($n = 7$)	7.91

Fig. 3. Examples of zircons from igneous and metasedimentary rocks with $^{207}Pb/^{206}Pb$ ages (Ma) and $\delta^{18}O$ values. Dashed white line follows core/rim boundaries. Locations of ion probe spots are shown with circles.

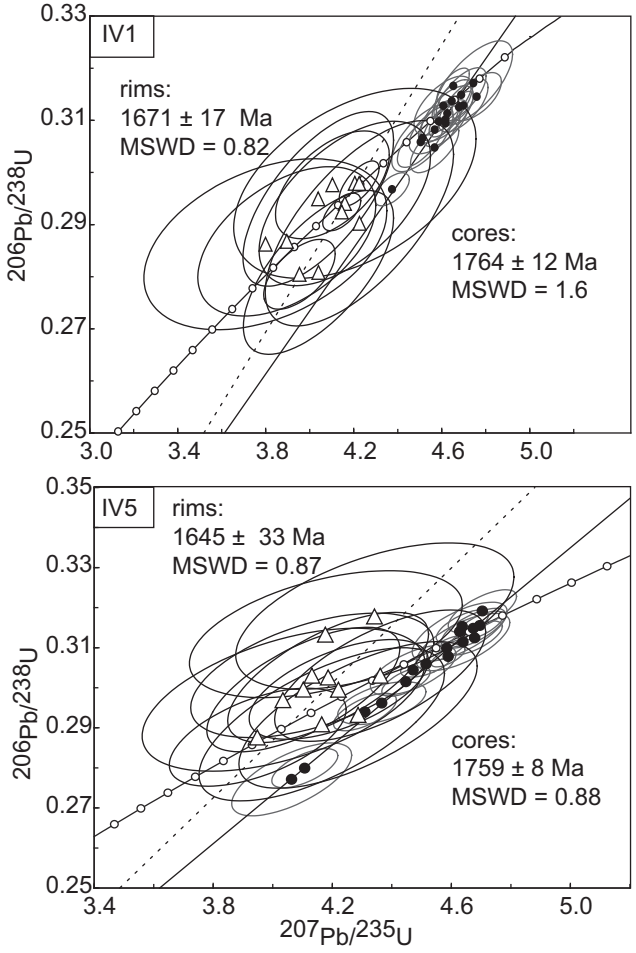

Fig. 4. U–Pb concordia diagrams for samples IV1 and IV5 of metagabbro from the Ivanpah Mountains. Low precision on the ages of the metamorphic overgrowths is due to low-U concentration.

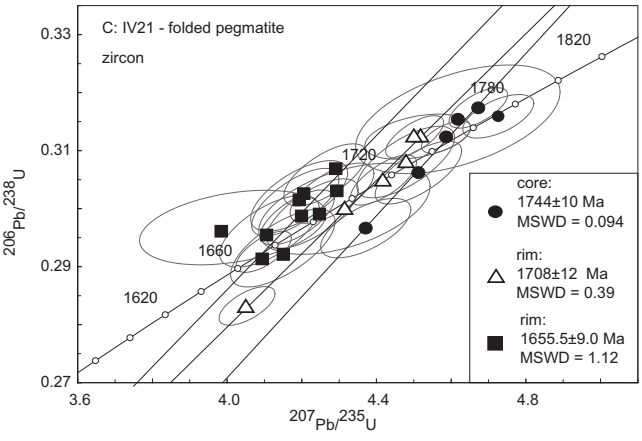

Fig. 5. Concordia diagram for zircons from a folded pegmatite, sample IV21. A crystallization age of 1744 ± 10 Ma is preserved in the oscillatory zoned cores (Fig. 3). Metamorphic overgrowths form two age populations at 1708 ± 12 and 1656 ± 9 Ma.

(sample IV41). The leucosome is coarse grained, biotite-bearing with only sparse garnets along the margin of the leucosome. Sample IV40 contains the assemblage quartz + plagioclase + K-feldspar + biotite + garnet. Forty-six analyses of zircons from IV40 are shown in Fig. 6A. These analyses are strongly discordant due to Pb loss, and poorly define a linear array with an upper intercept of 1737 ± 18 (MSWD = 18). This is interpreted as the crystallization age for the leucosome. No metamorphic zircon overgrowths were identified in this sample. However, monazites from this sample produce an upper intercept age of 1665 ± 7 (MSWD = 1.8) (Fig. 6B). However, we note that 6 out of 26 monazite analyzed were 1732 ± 8 to 1789 ± 5 Ma (Fig. 6B, Appendix 3), and are the same as the zircon age within error. This leucosome could be the same age as the gabbro, tonalite, augen gneiss suite with both zircon and monazite growing at the time of crystallization, and was affected by metamorphism at 1665 Ma when monazite grew.

Sample IV45 is a garnet-bearing leucocratic dike from the southern Ivanpah Mountains (Fig. 2C). It is coarse grained and contains garnet, quartz, plagioclase, and K-feldspar and appears undeformed (Fig. 2C). It trends N17W along strike and crosscuts the dominant, N–S-trending foliation along a sharp contact (Fig. 2C). Zircons from IV45 are large (>200 μm), euhedral and have crude oscillatory zoning. Fig. 6C shows a concordia diagram for zircons from the cross-cutting dike. Strongly discordant analyses are due to Pb loss as a result of higher U content (up to 5900 ppm). The concordia upper intercept age of 1663 ± 6 Ma is interpreted as the crystallization age of the dike (Fig. 6C). Monazites from sample IV45 are large and euhedral, and produced a concordia intercept age of 1666 ± 5 Ma (Fig. 6D).

Sample IV95 was collected ~100 m from IV40 (Fig. 1). It is a leucocratic, biotite-bearing granite dike ~1 m thick that is concordant with the migmatitic layering. It is coarse grained and contains quartz, plagioclase, K-feldspar and biotite; garnet is conspicuously absent. Similar to sample IV40, zircons from IV95 are strongly discordant due to Pb loss (Fig. 6E). They define a concordia intercept age of 1730 ± 25 Ma, and although imprecise, this is interpreted as the crystallization age. No younger, zircon overgrowths were identified.

Sample IV96 is from a cross-cutting, garnet-bearing leucocratic dike (Fig. 1). This dike strikes N15°E and crosscuts the garnet–biotite gneiss at a low angle. It is medium to coarse grained, equigranular, and contains quartz, plagioclase, K-feldspar and garnet, and appears undeformed. Analyses of zircon from IV96 form a linear array on a concordia diagram (Fig. 6F) with an upper intercept of 1661 ± 9 Ma (MSWD = 2).

In summary, three generations of igneous rocks have been identified in the Ivanpah Mountains: tonalite, augen gneiss, and metagabrro that were formed at 1760 Ma, pegmatites that intruded ca. 1740 Ma that are now deformed, and garnet-rich pegmatites intruded at 1670 Ma that appear undeformed.

6. Paragneisses

6.1. Detrital zircons from paragneisses

Detrital zircons are abundant in the paragneisses from the Ivanpah Mountains. Zircons from the paragneisses are typically comprised of oscillatory zoned interiors mantled by narrow, unzoned overgrowths (Fig. 3). Analyses of zircon cores yield a distinctive detrital age population, and Fig. 7 shows a histogram of $^{207}Pb/^{206}Pb$ ages from 180 zircon interiors from five samples of paragneiss. Determination of the youngest detrital grain from each sample (Table 2) was based on $^{232}Th/^{238}U$ values, and the analysis location (i.e. core, rim, oscillatory zoned section). Analyses greater than 15% discordant are excluded. The youngest detrital zircon age from each sample ranges from 1754 ± 24 to 1794 ± 16 Ma (Table 1). The majority of the detrital ages are between 1.8 and 2.0 Ga (Fig. 7). Few detrital zircon ages from ~2.1 to 2.5 Ga were identified, but a secondary population of detrital zircons ranges from 2.5 to 2.9 Ga (Fig. 7). This age pattern is identical to detrital zircon ages reported from the San Bernardino Mountains in the western Mojave Province (Barth et al., 2000, 2009), and detrital zircons from the Vishnu Schist

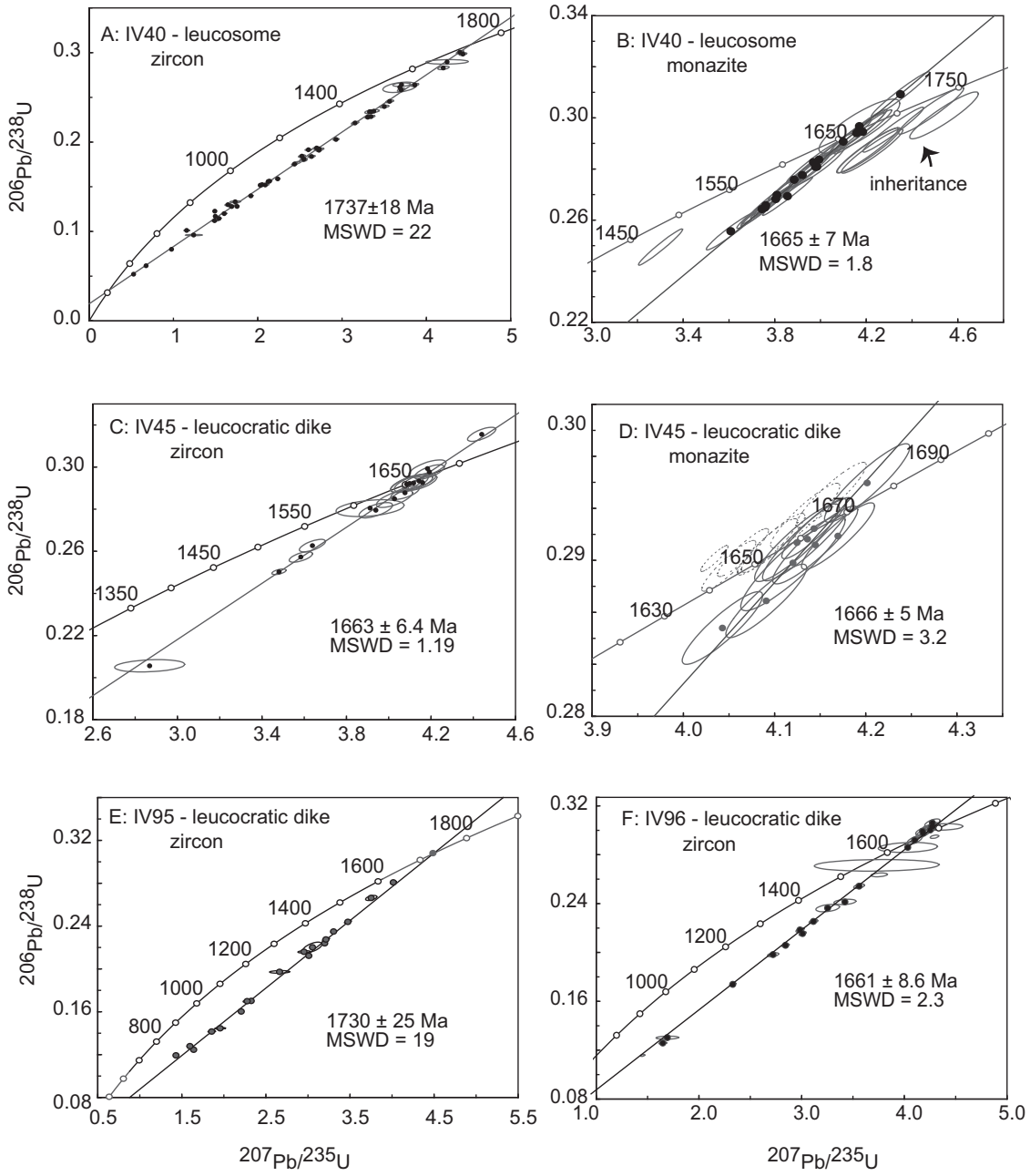

Fig. 6. Concordia diagrams for zircon and monazite from leucocratic rocks from the Ivanpah Mountains. A) Zircon age determined for sample IV40, a folded leucosome. B) Monazite results from IV40. C) Zircon results from sample IV45, a garnet-bearing dike. D) Monazite analyses from IV45. E) U–Pb zircon results from IV95, and garnet-bearing dike. F) U–Pb zircon concordia diagram for results from sample IV96, a biotite-bearing sill. See text for discussion.

in Grand Canyon (Shufeldt et al., 2010), which suggests widespread deposition of sediments with this provenance.

6.2. U–Pb geochronology of zircon overgrowths (rims)

Detrital zircon grains in the paragneisses from the Ivanpah Mountains have overgrowths that preserve a complex record of polyphase metamorphism. In cathodoluminescence, the overgrowths on the detrital zircon grains are typically dark and unzoned or have only crude oscillatory zonation (Fig. 3). Zircon overgrowths from five samples of garnet–biotite gneiss and one sample of quartzite were analyzed for U–Pb geochronology.

Sample IV22 was collected from the central Ivanpah Mountains (Fig. 1) and is a microcrystalline, aluminous, quartzite with minor garnet and fibrolitic sillimanite. Its metasedimentary origin is indicated by its detrital zircon population (Fig. 7). Zircon overgrowths are poorly developed in this sample, but 10 analyses of narrow zircon overgrowths produced a linear array on concordia with an upper intercept of 1760 ± 18 Ma (Fig. 8A). The $^{232}Th/^{238}U$ ratio of these analyses ranges from 0.41 to 0.0045 (Appendix 2), which is consistent with metamorphic growth.

Sample IV41 is a sample of garnet–biotite paragneiss from a small hill located in the southern Ivanpah Mountains (Fig. 1) and represents the host gneiss for the leucosome sampled as IV40. Sample IV41 contains garnet, biotite, fibrolitic sillimanite, K-feldspar, plagioclase, quartz and cordierite, and as with all the garnet–biotite gneisses, sample IV41 has a pervasive migmatitic layering of leucosome and melanosome at all scales. Numerous garnets are concentrated in the biotite-rich melanosomes. Sillimanite and biotite form a poorly developed foliation that is deflected around

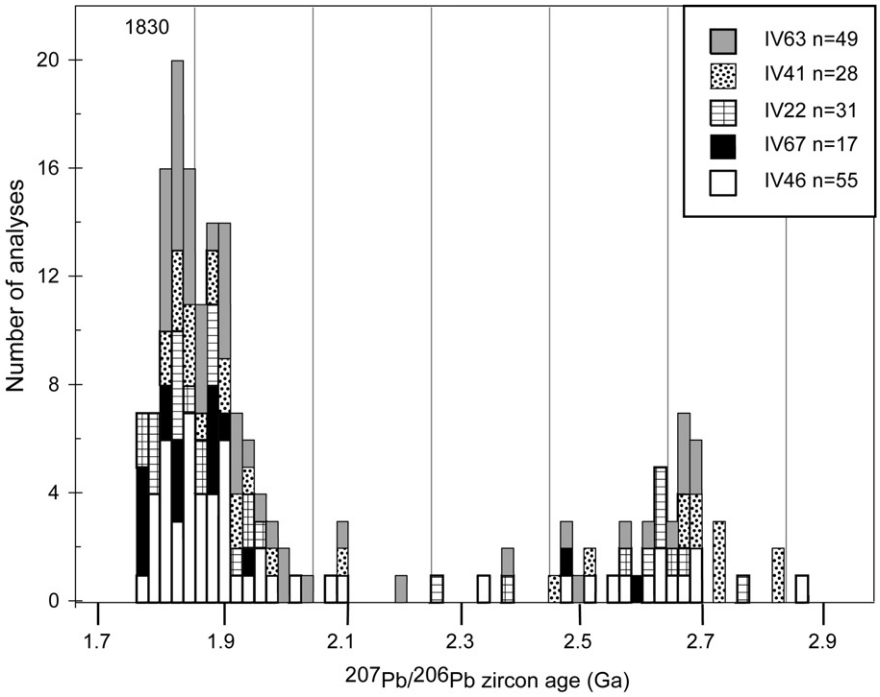

Fig. 7. Detrital zircon $^{207}Pb/^{206}Pb$ ages from zircon interiors from five samples of paragneiss from the Ivanpah Mountains. Analyses that are greater than 15% discordant are not shown. Inset shows two representative zircon grains that have oscillatory zoned cores with thin, grey, metamorphic rims.

the garnets, and the garnets do have crude pressure shadows of quartz and biotite. These observations are taken to indicate that the garnets in this sample are late syn-deformational with respect to the main foliation, which is likely a composite foliation that transposed earlier fabrics. Metamorphic overgrowths on detrital zircons from sample IV41 have $^{232}Th/^{238}U$ ratios of 0.01–0.48 (Appendix 2), and $^{207}Pb/^{206}Pb$ ages range from 1774 ± 10 to 1658 ± 14 Ma. The analyses cluster onto two groups at 1760–1730 and 1710–1680 Ma (Fig. 8B), which may reflect two periods of metamorphic zircon growth. However, no robust age determinations could be made.

IV46 is from the garnet–biotite paragneiss collected from the southern Ivanpah Mountains where it was found cut by an undeformed, leucocratic dike (sample IV45) (Fig. 2C). Sample IV46 has the same mineral assemblage and texture as IV41. Analyses of metamorphic zircon overgrowths from sample IV46 form a population with a concordia intercept age of 1702 ± 7 (MSWD = 0.77) with two older and one younger analyses excluded (Fig. 8C). The $^{232}Th/^{238}U$ ratio of these analyses is very low and ranges from 0.2 to 0.02 (Appendix 2), which is indicative of metamorphic growth.

Samples IV63 and IV65 are garnet–biotite gneisses from the central Ivanpah Mountains (Fig. 1). Both samples contain garnet, biotite, K-feldspar, plagioclase, quartz, cordierite and fibrolitic sillimanite. Samples IV63 and IV65 are from the same outcrop and represent more leucocratic and restitic versions of the migmatitic layering, respectively. Twenty-six analyses of zircon overgrowths from sample IV63 produced a spread of concordant ages from 1647 ± 13 to 1765 ± 22 Ma (Fig. 8D). The $^{232}Th/^{238}U$ ratios of the zircon overgrowths from sample IV63 range from 0.02 to 0.73 (Appendix 2). The majority of the zircon analyses are ~1.70 Ga, however, the concordia diagram shown in Fig. 8D illustrates the continuous spread of zircon overgrowth ages from 1647 ± 13 to 1765 ± 11 Ma in this sample. Therefore, a single robust age determination was not made.

Sample IV65 is the leucosome-poor, biotite-rich, restitic version of the garnet–biotite gneiss that was collected less than 1 m from sample IV63 (Fig. 1). U–Pb analyses of zircon overgrowths from IV65 mostly fall into one cluster on a concordia diagram (Fig. 8E), and 13 out of 16 analyses of overgrowths yield a concordia intercept age of 1665 ± 9 Ma (MSWD = 0.79). Three analyses of zircon overgrowths are slightly older and range from 1700 ± 19 to 1758 ± 10 Ma. The $^{232}Th/^{238}U$ ratios of the zircon overgrowths from sample IV65 range from 0.04 to 0.49 (Appendix 2).

Sample IV67 is a coarse grained version of the garnet–biotite gneiss from the central Ivanpah Mountains (Fig. 2C). Twenty-five analyses of metamorphic overgrowths from IV67 are shown in Fig. 8F, and 19 analyses define a liner array with an upper intercept at 1738 ± 20 Ma (MSWD = 3.9). The remaining six analyses define a concordia intercept age of 1659 ± 23 (MSWD = 2.1). No difference between the two populations was noticeable in CL. The $^{232}Th/^{238}U$ ratios of the ca. 1.74 Ga zircon are restricted to a narrow range of 0.03–0.11, whereas the younger population of zircon has $^{232}Th/^{238}U$ ratios that range from 0.03 to 0.77 (Appendix 2). In contrast to the other metasedimentary samples, analyses of zircon overgrowths from this sample indicate two distinct periods of metamorphic zircon growth.

Fig. 9A shows a histogram and probability density curve of $^{207}Pb/^{206}Pb$ ages from zircon overgrowths from the paragneisses of the Ivanpah Mountains ($N = 113$). Analyses that are greater than 10% discordant were excluded. The ages are spread over more than 100 million years with poorly defined peaks ca. 1.73, 1.71, and 1.68 Ga. Due to the precision of these analyses, typically on the order of ±10–15 m.y. (2σ), many of the zircon ages are overlapping in uncertainty.

6.3. Monazite in the paragneisses

Monazite is a useful chronometer because it participates in metamorphic reactions from greenschist to granulite facies and will grow during metamorphism at far lower temperatures zircon. Monazite is well known for its ability to preserve multiple age domains and for it's ability to dissolve and reprecipitate during metamorphic reactions among other phases or ductile deformation (Pyle and Spear, 2003; Kohn and Malloy, 2004). The paragneisses from the Ivanpah Mountains contain abundant monazite often

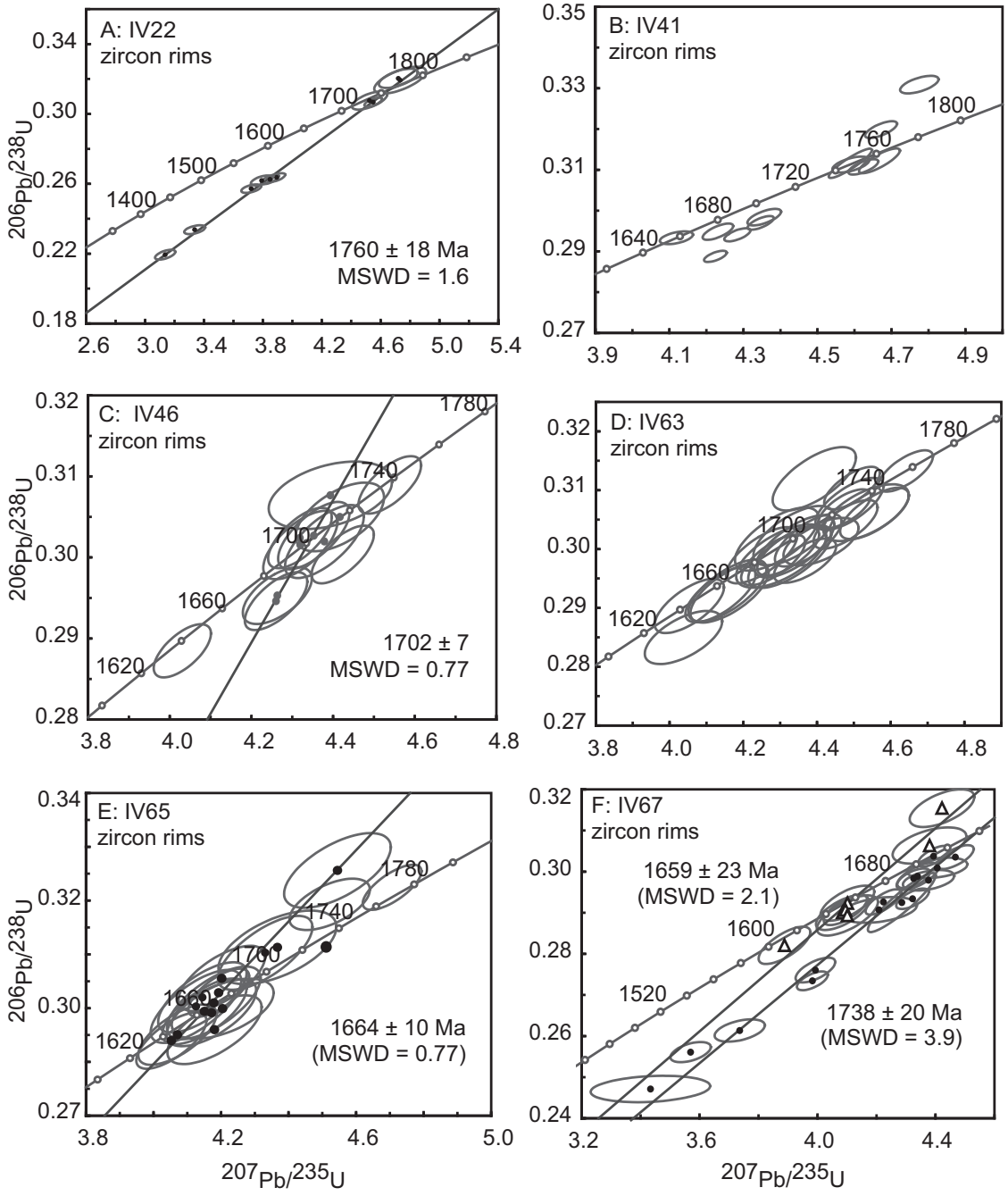

Fig. 8. A–F) Concordia diagrams for metamorphic zircon from paragneisses in the Ivanpah Mountains. Sample IV22 is an aluminous quartzite, and all others are from garnet + biotite + K-feldspar + plagioclase + quartz + sillimanite + cordierite-bearing gneiss.

as large (>100 μm), euhedral to subhedral grains that are clearly visible in thin section. Monazite is present in these samples both as inclusions within major minerals (e.g., garnet) and in the matrix. In BSE imaging (Fig. 10), these grains are commonly zoned with complex or patchy zonation, and many contain discrete growth domains as cores and overgrowths that correspond to different ages.

Fig. 11A–E show the concordia diagrams for analyses of monazites from five samples of paragneiss that were discussed in Section 6.2. Analyses of monazite from each sample produced a strongly bimodal distribution of ages, which is strikingly different from the results of the zircon overgrowths. The concordia ages for first period of monazite growth range from 1748 ± 4 to 1739 ± 10 Ma (Fig. 11). The presence of monazite cores of this age suggests that this was the first metamorphic event that produced widespread monazite in these rocks.

The second period of monazite growth occurred between 1680 ± 3 and 1665 ± 12 Ma (Fig. 11). Monazite of this age occurs as overgrowths on composite grains, and as whole crystals (Fig. 10). The histogram in Fig. 9B is a compilation of 183 monazite analyses from all samples. The results indicate two distinct periods of monazite growth ca. 1748 and 1672 Ma. A younger period of monazite growth may have occurred ca. 1640 Ma, although these younger ages may be the result of disturbance by hydrothermal fluids at ca. 1.4 Ga related to the Mountain Pass mineralization.

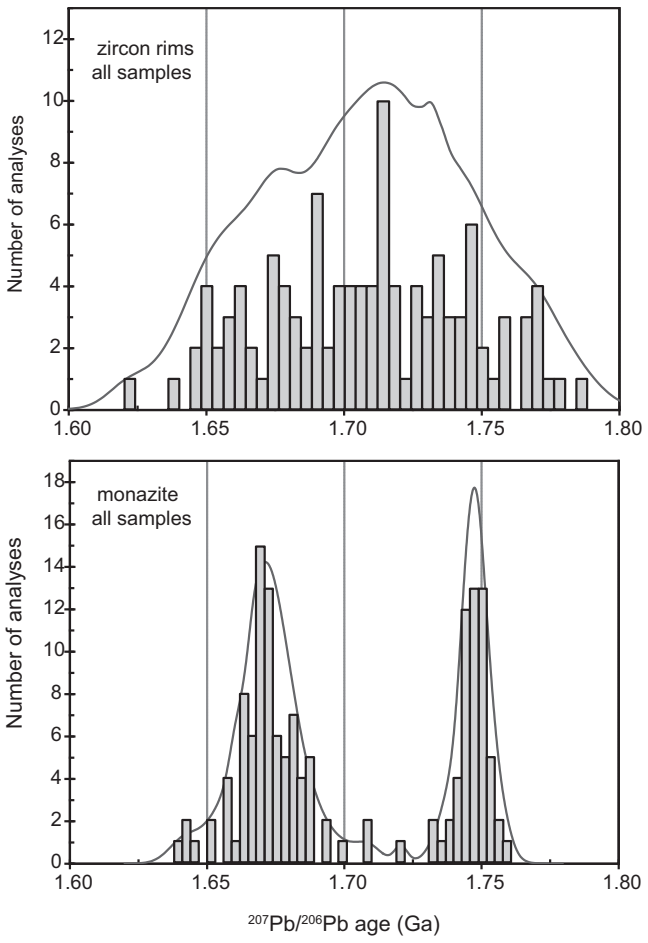

Fig. 9. Histograms and probability curves for U–Pb zircon and monazite data. Analyses that are greater than 15% discordant are not shown. A) $^{207}Pb/^{206}Pb$ ages of zircon metamorphic from six samples shown in Fig. 8 ($n = 113$). B) $^{207}Pb/^{206}Pb$ ages of monazite for five samples shown in Fig. 11 ($n = 183$).

6.4. In situ monazite ages

In an attempt to characterize the spatial distribution of the two age populations of monazite in the paragneisses, samples IV41 and IV46 were selected for in situ monazite age determinations (Fig. 12 and Table 3). Polished rock chips were prepared and carefully imaged in BSE, then energy dispersive X-ray analyses was used to identify the monazites and their host minerals prior to U–Pb analyses. A total of 29 monazites from the two samples were large enough to be analyzed (15–30 μm) (Table 3). Some zonation in the monazites was observed but difficult to image given their small size. Several zircons were identified in situ, but all were too small (<10 μm) to be analyzed.

The in situ monazite analyses produced a range of ages from 1.75 to 1.65 Ga, and are not as strongly bimodal as the analyses of monazite separates (Fig. 12). The likely reason is that the when grains are cast into epoxy mount, care is taken to select large grains and expose equatorial section of the grains, therefore providing the maximum possible analytical space. Therefore it is often possible to place the beam on cores and rims without overlapping. The monazite grains that were analyzed in situ were small (15–30 μm), and any age domains would have been unavoidable by the ion beam (~15 μm), leading to mixed ages. Ten monazite inclusions in garnet were analyzed and ranged in age from 1665 ± 12 to 1741 ± 6 Ma, which is nearly identical to the range of monazite ages found in the matrix (Table 3). Only two monazite grains were found as an inclusion in cordierite, and they yielded a $^{207}Pb/^{206}Pb$ age of 1697 ± 8 and 1719 ± 10 Ma. The presence of 1.65–1.67 monazite grains included in garnet, K-feldspar, and biotite suggests that the current mineral assemblage and texture formed at or after that time. This is supported by the fact that the ages of the matrix monazite are the same as monazite included in minerals (Fig. 12).

7. Thermobarometry

Spectacular, large garnets are ubiquitous in the garnet–biotite gneisses (Fig. 2). Many are euhedral to subhedral and inclusion-rich. Large quartz inclusions are common, and the garnets also contain inclusions of plagioclase, K-feldspar, biotite, sillimanite, monazite and zircon. Interestingly, no inclusions of cordierite were identified

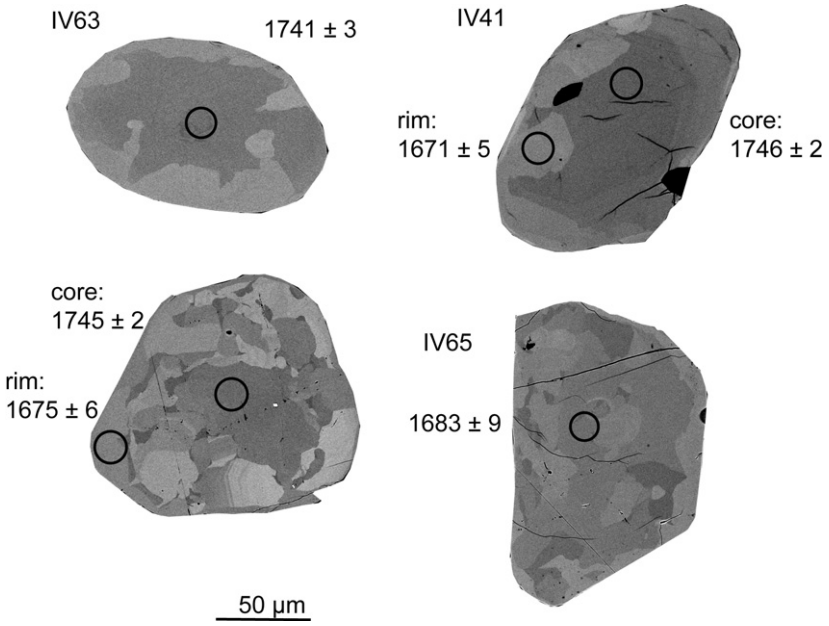

Fig. 10. Examples of monazite grains and textures in BSE. Locations of SHRIMP spots are shown with black circles and correspond to the $^{207}Pb/^{206}Pb$ ages shown.

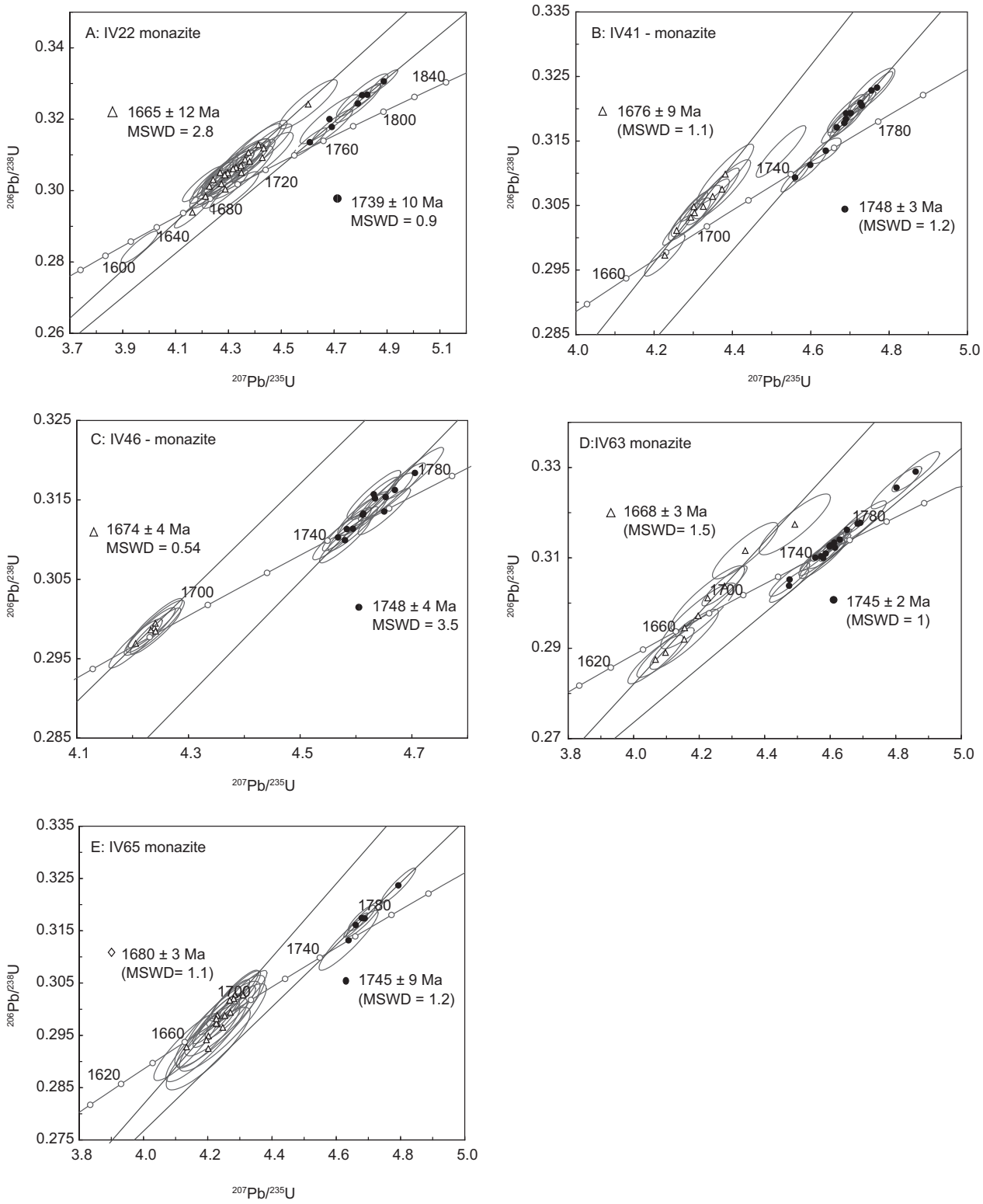

Fig. 11. A–E) Concordia diagrams for monazite from paragneisses in the Ivanpah Mountains. Sample IV22 is an aluminous quartzite, and all others are from garnet + biotite + K-feldspar + plagioclase + quartz + sillimanite + cordierite-bearing gneiss.

in garnet although cordierite is abundant in the matrix assemblage. The garnets are almandine-rich and nearly homogeneous in major element composition (Appendix 4).

Garnet, biotite, cordierite and plagioclase chemistries were analyzed in samples IV41 and IV46 by electron microprobe and the Program GTB (Kohn and Spear, 2003) was used to calculate garnet–biotite thermometry and GASP barometry (Fig. 13; Appendix 4). Both samples contain the major mineral assemblage: garnet + biotite + quartz + K-feldspar + cordierite + sillimanite + plagioclase. Hodges and Spear (1982) was used for GASP barometry and garnet–biotite thermometry. The calibration of Nichols et al. (1992) was used for garnet–cordierite–sillimanite–quartz

Table 3
Results from in situ U–Pb analyses of monazite from samples IV41 and IV46.

Interstitial	% comm 206	ppm U	ppm Th	$^{232}Th/^{238}U$	Age Ma 207/206 Uncorr	Error Ma 2σ
IV46B-6	0.06	1075	16,469	15.8	1651	8
IV46B-2	0.08	1069	17,067	16.5	1701	8
IV41B-24	0.39	315	21,375	70.1	1665	16
IV41B-6	0.16	1387	60,347	45.0	1686	26
IV41B-21	0.07	1306	22,962	18.2	1704	10
IV41B-20	0.07	1865	21,667	12.0	1724	6
IV41B-3	0.09	1897	26,664	14.5	1740	8
IV41B-10	0.04	2678	19,652	7.6	1753	6
In garnet						
IV46B-7	0.07	1404	15,520	11.4	1679	6
IV46B-1	0.29	1113	16,023	14.9	1724	8
IV46B-9	0.06	1681	19,030	11.7	1692	8
IV46B-11	0.04	1670	16,081	9.9	1719	6
IV46B-12	0.06	1367	19,161	14.5	1746	6
IV46B-13	0.04	3150	14,595	4.8	1746	4
IV46B-10	0.03	2145	16,726	8.1	1746	6
IV41B-22	0.22	487	18,924	40.2	1665	12
IV41B-18	0.06	2297	21,152	9.5	1733	10
IV41B-23	0.08	1754	26,044	15.3	1745	8
In quartz						
IV46B-8	0.06	1071	16,128	15.6	1682	8
IV46B-5	0.05	1534	16,846	11.3	1684	6
IV46B-15	0.07	1172	17,738	15.6	1744	8
IV41B-1	0.02	1702	7616	4.6	1665	8
IV41B-4	0.05	2808	25,540	9.4	1750	6
In K-feldspar						
IV46B-3	0.10	850	17,298	21.0	1660	10
IV41B-20	0.13	1089	19,994	19.0	1706	8
IV41B-12	0.03	3480	20,224	6.0	1748	4
In cordierite						
IV41B-13.2	0.17	1062	21,793	21.2	1697	8
IV41B-13	0.19	953	22,564	24.5	1719	10
In biotite						
IV41B-11	0.28	868	19,957	23.7	1714	10

barometry. Several crystals from each sample were analyzed multiple times, and the averages for each crystal were randomly paired and used in the thermobarometry. Total Fe was assumed to be ferrous. Sample IV46 yields temperatures of 670–740 °C with a corresponding GASP pressure of 2.1–4.2 kb (shaded area on Fig. 13) and a corresponding cordierite–garnet pressure of 3.1–4 kb. Sample IV41 yields temperatures of 740–780 °C with a corresponding GASP pressure of 3–4 kb. Although sample IV46 seemingly yields lower temperatures than sample IV41, the lowest temperature estimate from IV41 corresponds to the highest temperature estimate from sample IV46 (~740 °C), and given an error 30–50 °C, these two samples could be showing a very similar result. However, these samples were collected ~1 km apart from each other and a real temperature gradient is possible, or alternatively, sample IV46 may have experienced some retrogression. We conclude that peak metamorphism in the Ivanpah Mountains occurred at ~740 °C and 3.5 kb at about 1.65–1.67 Ga.

8. Oxygen isotopes in zircon

Oxygen isotope ratios were determined from the same grains that were dated by U–Pb analysis by using the IMS-1280 housed at the University of Wisconsin. The oxygen analysis pits were placed adjacent to U–Pb pits in the same CL zone (see Appendices A and 5). Detrital zircons in the metasedimentary rocks show a significant difference between the two main detrital age populations (Figs. 7 and 14). The Archean cores have $\delta^{18}O$ values of 6.3 ± 1.4‰ (n = 14) (Fig. 14), which is consistent with $\delta^{18}O$ of Archean igneous zircons values worldwide (Valley, 2003; Valley et al., 2005). Rare Archean zircons with $\delta^{18}O > 7.5$ are likely metamorphic in origin based on their Th/U ratios (Appendix 2). The 2.0–1.8 Ga detrital zircon suite has variable $\delta^{18}O$ values (Fig. 14) that range from mantle-like values as low as 4‰ to more evolved values; most are below 8.5‰ but one analysis is above 10‰ (Fig. 14, Appendix 5). The values of $\delta^{18}O$(zircon) from the younger population suggest a variety of lithologies in the source area, most of which were continental, which would be consistent with known orogenic belts of this age (e.g., Trans Hudson orogeny). The preservation of original, magmatic $\delta^{18}O$ values in the detrital zircon cores indicates that oxygen isotope ratios in zircon can be preserved despite partial melting of the enclosing rock (Valley et al., 1994; Peck et al., 2003; Page et al., 2007; Bowman et al., 2011).

Oxygen isotope ratios were determined in the zircon overgrowths of the metaquartzite (sample IV22), four samples of garnet–biotite gneiss (samples IV41, IV46, IV63 and IV67), and four leucocratic rocks (samples IV21, IV40, IV45 and IV96). Fig. 15A shows the age of zircon metamorphic overgrowths from the paragneisses vs. the corresponding $\delta^{18}O$ values, and Fig. 15B shows the results from igneous, leucocratic rocks. On Fig. 15, in samples for which we determined discrete ages from zircon (samples IV21, IV22, IV40, IV45, IV46, and IV67; Figs. 5, 6 and 8), we assigned their concordia intercept ages to the corresponding oxygen isotope analysis. For samples IV41 and IV63, the ^{204}Pb corrected, $^{207}Pb/^{206}Pb$ age of each spot was paired with the corresponding oxygen isotope analysis. In general, the $\delta^{18}O$ values of metamorphic zircon overgrowths from the paragneiss samples do not show a strong correlation with age (Fig. 15, Appendix 5). The $\delta^{18}O$ values of the metamorphic zircon overgrowths in a given

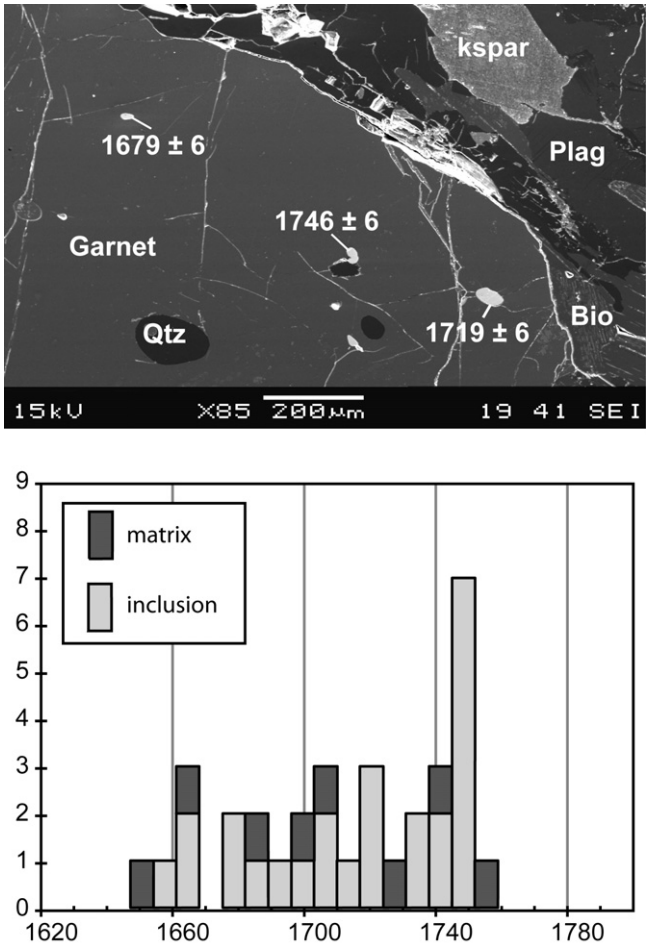

Fig. 12. In situ monazite results. A) Large garnet in BSE showing monazite inclusions and their $^{207}Pb/^{206}Pb$ ages. B) Histogram of in situ monazite ages. Filled boxes are from monazites in the matrix while open box are from monazites included in other minerals.

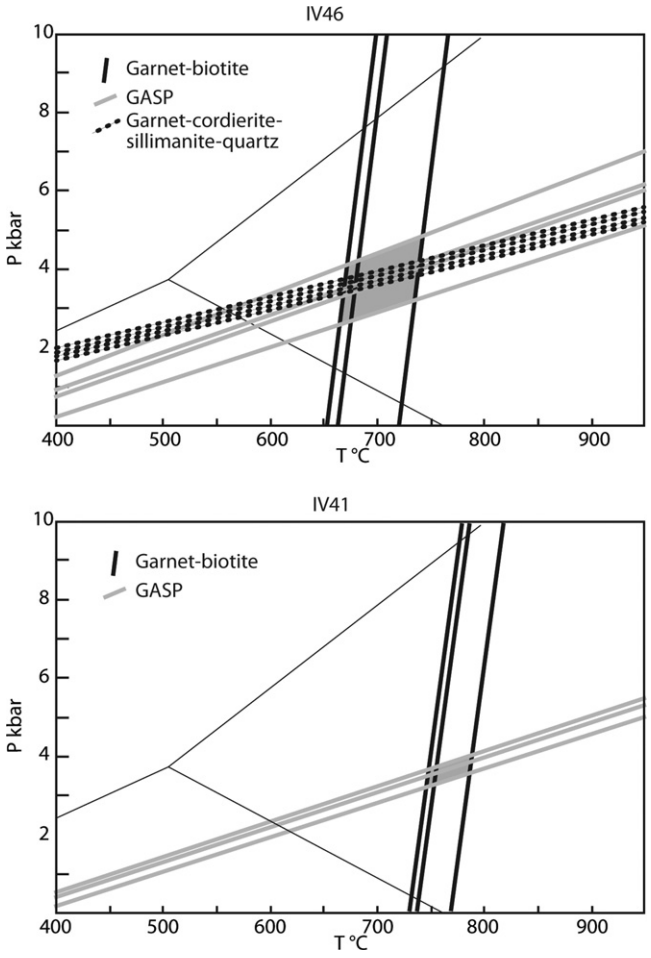

Fig. 13. Pressure–temperature conditions from Ivanpah Mountains determined with garnet–biotite thermometry, GASP barometry (Hodges and Spear, 1982) and garnet–cordierite–sillimanite–quartz barometry (Nichols et al., 1992). Peak metamorphic conditions are indicated by the shaded areas. A) Shows results for sample IV46 and B) shows results from sample IV41.

sample are less variable in isotopic compositions than the detrital cores.

The zircons from the metaquartzite, sample IV22, contain 1.76 Ga overgrowths that have a bimodal distribution of $\delta^{18}O$(zircon) values of 9.0 ± 0.9‰ and 6.3 ± 0.5‰ (2SD). This is consistent with heterogeneity in the sedimentary layering of the host rock. The detrital zircon cores from this sample have $\delta^{18}O$ values that range from 5.2‰ to 8.4‰ (Fig. 7, Table 2). This relation is true of the younger metamorphic overgrowths as well; the oxygen isotope ratios of the detrital cores are unrelated to the oxygen isotope ratios of the metamorphic overgrowths.

The metamorphic zircon overgrowths from sample IV63 yield a continuous spread on concordia of U–Pb zircon ages, and the overgrowths have an average $\delta^{18}O$ value of 9.7 ± 0.6‰ (n = 9, 2SD) through time (Fig. 14). Similarly, sample IV46 also contains zircons that maintain a relatively constant $\delta^{18}O$ value over time with an average of 10.5 ± 0.4‰ (n = 9, 2SD). The ca. 1.74 Ga metamorphic zircon overgrowths in sample IV41 have the lowest $\delta^{18}O$(zircon) values of all the paragneiss samples with an average of 6.8 ± 1‰ (n = 8, 2SD) (Fig. 14). Sample IV67 showed two age populations of metamorphic zircon overgrowths at 1659 ± 23 and 1738 ± 20 Ma which yielded $\delta^{18}O$ values of 9.3 ± 1.2‰ (n = 13, 2SD) and 7.7 ± 0.5‰ (n = 7, 2SD), respectively.

Zircons from four samples of igneous rock were analyzed for oxygen isotope ratios. Sample IV40 is a deformed, 1.74 Ga leucocratic rock that is interlayered with sample IV41 of the garnet–biotite

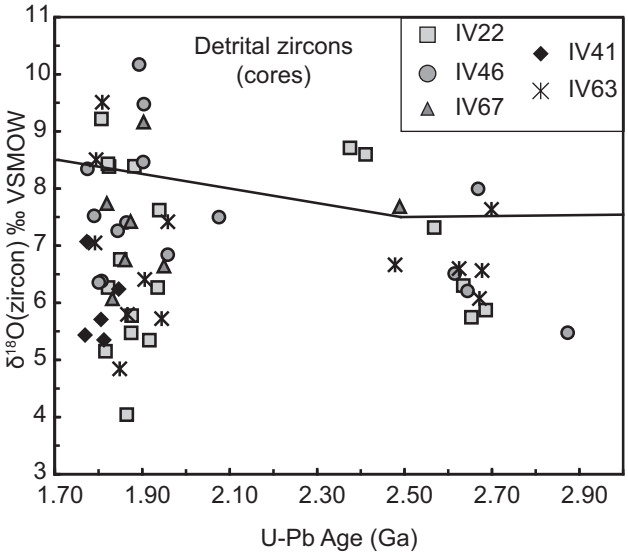

Fig. 14. $\delta^{18}O$ values for the detrital zircon cores from five samples of metasedimentary rocks from the Ivanpah Mountains. Line shows approximate upper value for igneous zircons from Valley et al. (2005).

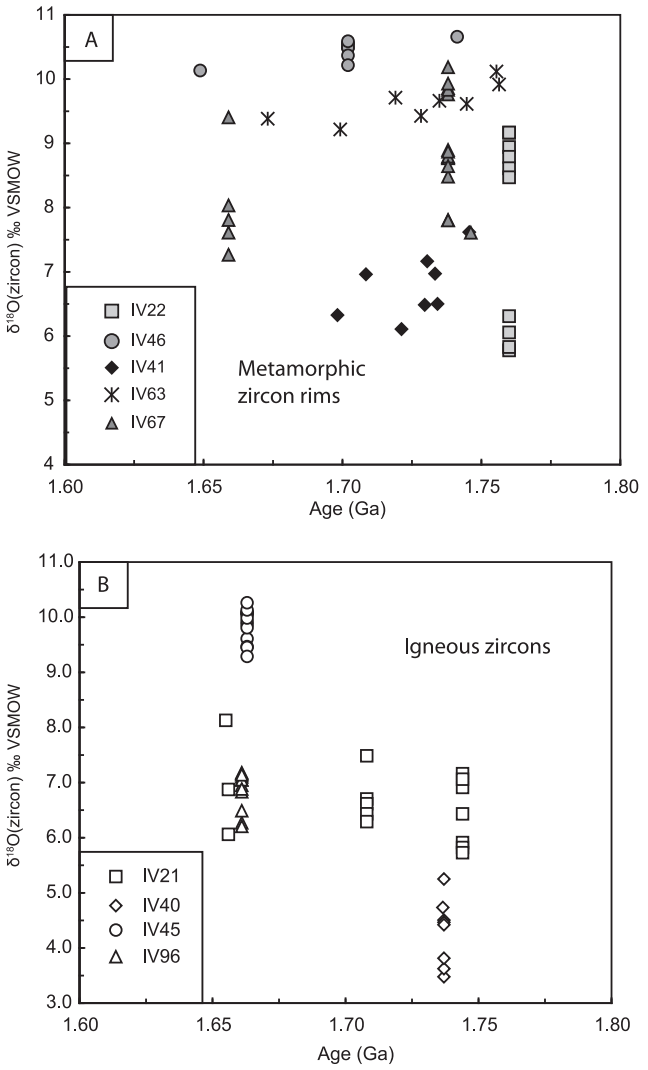

Fig. 15. Age distribution of $\delta^{18}O$ values from metamorphic zircon overgrowths. For samples with concordia intercept ages, the age assigned to the corresponding $\delta^{18}O$ values is the intercept age. For samples with a spread of U–Pb zircon ages for which an age could not be determined (IV41, and IV63), the ^{204}Pb corrected, $^{207}Pb/^{206}Pb$ age was used. Samples IV40 and IV41 represent a leucosome–melanosome pair. Sample IV46 is a garnet–biotite gneiss that is crosscut by a leucocratic dike, sample IV45. Samples IV67 and IV63 are from the garnet–biotite gneiss. Sample IV21 is a pegmatite that intruded granitic gneiss at 1.74 Ga, and the zircons preserve metamorphic growth at 1.70 and 1.66 Ga.

gneiss. Sample IV40, had the lowest $\delta^{18}O$(zircon) values of all the samples, with an average of 4.3 ± 0.6‰ ($n = 8$, 2SD). The host gneiss, sample IV41, had much higher $\delta^{18}O$(zircon) overgrowth values of 7.3 ± 0.9‰ ($n = 7$, 2SD) at the time of intrusion (Fig. 15). The differences between the $\delta^{18}O$(zircon) values for samples IV40 and IV41 indicate that the leucosome could not have been generated in a closed system by in situ partial melting alone. Therefore, the deformed leucosome likely intruded the garnet–biotite gneiss at 1.74 Ga.

Sample IV45 is a 1.66 Ga leucocratic dike that crosscuts sample IV46 of the garnet–biotite gneiss (Fig. 2). The $\delta^{18}O$(zircon) average value from the cross-cutting dike, IV45, is 9.9 ± 0.3‰ ($n = 14$, 2SD; Fig. 14), which is higher than the $\delta^{18}O$(zircon) average of the metamorphic zircon overgrowths of the same age in the paragneiss, suggesting that the dike was not formed by in situ partial melting of the host rock.

Sample IV21 is a deformed pegmatite with zircons that preserve three ages of growth; the igneous cores are ca. 1.74 Ga, and two periods of zircon growth occurred at ca. 1.70 and 1.66 Ga. These periods of growth correspond to $\delta^{18}O$(zircon) average values of 6.4 ± 1.2 ($n = 7$, 2SD), 6.7 ± 0.9 ($n = 5$, 2SD) and 7.0 ± 2.1 ($n = 3$, 2SD), respectively (Fig. 15).

Sample IV96 is from a cross-cutting, garnet-bearing leucocratic dike with a U–Pb age of 1661 ± 9 Ma. Zircon from this sample has a $\delta^{18}O$ average value of 6.9 ± 0.3 ($n = 12$) and are similar to the $\delta^{18}O$ values from sample IV21, the deformed pegmatite.

Laser fluorination of garnets was performed on four metaigneous rocks and five metasedimentary rocks (Tables 1 and 2). In each sample, except for IV45, the laser fluorination $\delta^{18}O$ value for the garnet matches the SIMS $\delta^{18}O$ values for the zircon metamorphic overgrowths. This relation is taken to indicate that the garnet was in equilibrium with zircon when it grew ($\Delta^{18}O$(zircon–garnet) ~0‰ at ~740 °C). Just like for the zircons, the different $\delta^{18}O$ values between different garnets reflects the original heterogeneity of the sedimentary deposits.

In summary, oxygen analysis of the zircons from the paragneisses shows that the detrital cores of the zircons preserve their original $\delta^{18}O$ values despite likely partial melting of the enclosing rock. The $\delta^{18}O$ values of metamorphic overgrowths on zircons from the paragneisses are consistent with in situ partial melting during each period of metamorphic zircon growth, whereas $\delta^{18}O$(zircon) values from leucocratic rocks are significantly different than in the host gneiss, indicating an intrusive relation. The consistency of $\delta^{18}O$ values within paragneiss samples through time, particularly samples IV63 and IV46 (Fig. 15) suggests that the oxygen isotope ratios in the metamorphic zircons reflect the whole rock $\delta^{18}O$ values of each sample, and this variation from sample to sample reflects original stratigraphic heterogeneity.

9. Discussion

9.1. Zircon vs. monazite behavior

Zircons and monazites from the paragneisses exposed in the Ivanpah Mountains record multiple periods of metamorphic growth, but the patterns of zircon ages differ between samples (Table 4). Several possibilities may explain the variation of zircon ages: (1) these zircons preserve a record of prolonged or repeated metamorphic growth during tectonic events from ca. 1.76 to 1.65 Ga, (2) the formation of metamorphic overgrowths on zircon first occurred at 1.74 Ga and was then variably overprinted by metamorphism at 1.67 Ga such that the intermediate ages ca. 1.70 Ga are partially reset, (3) the 1.74 and 1.67 Ga age domains in the zircon overgrowths are smaller than the resolution of the ion beam resulting in mixed/average ages at 1.70 Ga,

Table 4
Summary of tectonic events from the Ivanpah Mountains.

Age	Ivanpah Mountains	Igneous zircon	Zircon overgrowths	Monazite
Post 1.79 Ga	Deposition of sediments	Detrial		
1.76 Ga	Intrusion of augen gneiss, tonalite, gabbro suite	JW21, IV3, IV5	IV22	
1.74 Ga	Metamorphism and magmatism	IV21, IV40, IV95	IV67	All paragneiss samples
ca. 1.70 Ga	Metamorphism and deformation? (Ivanpah orogeny)		IV46, IV21	
1.67 Ga	Migmatization, pervasive metamorphic mineral growth, leucocratic dike intrusion	IV45, IV96	IV41, IV65, IV67, IV21	All paragneiss samples

(4) these samples were not spatially related before 1.67 Ga, and therefore had different *P–T* paths. The effects of the last possibility are difficult to discern, especially since upright, isoclinal folds and attenuated fold hinges are common, and similar garnet–biotite–sillimanite–cordierite-bearing paragneisses have been reported in the McCullough Mountains (Thomas et al., 1988; Young, 1989). The second and third possibilities, that the 1.70 Ga ages are isotopic mixtures either by partially resetting or finely intergrown age domains within the zircon overgrowths, would agree with the bimodal nature of the monazite ages, but several previous authors have reported ca. 1.70 deformation and metamorphism from the Mojave province (see Section 2; Wooden and Miller, 1990; Hawkins et al., 1996; Ilg et al., 1996; Duebendorfer et al., 2001; Bryant et al., 2001; Barth et al., 2009). Therefore, we prefer to interpret the 1.70 Ga metamorphic zircon ages as geologically real and further investigation is ongoing.

In stark contrast to the metamorphic zircon, monazite from the paragneisses records two ages, 1.67 and 1.74 Ga, with remarkable regularity (Figs. 9B and 11, Table 3; Appendix 3). Monazite grains analyzed from each sample are rounded, >100 μm in diameter, show a patchy zonation in BSE, and core and rim morphology is common (Fig. 9). The lack of 1.70 Ga monazite ages could indicate that monazite was being consumed or absorbed at this time. Where preserved, the monazite cores are irregular in shape and frequently embayed (Fig. 9), suggesting a period of monazite resorption and/or dissolution and re-precipitation. Pyle and Spear (2003) reported monazite resorption during prograde metamorphism that occurred at temperatures above ~750 °C along two simultaneous reactions which together produce garnet, K-feldspar, cordierite and melt. Another interpretation is that the monazite textures indicate simultaneous dissolution and re-precipitation of the monazite in the presence of metamorphic fluids, at 1.67 Ga. Experimental studies of monazite have shown that dissolution and re-precipitation of monazite is an effective mechanism for resetting the U–Pb isotopic system, especially in Ca and Pb-rich fluids (Seydoux-Guillaume et al., 2002). Although dissolution and re-precipitation of monazite may have occurred, the presence of abundant, large monazite crystals in the 1.66 Ga leucocratic dike, sample IV45, indicates that the melts and/or fluids were causing new monazite growth at that time.

9.2. Garnet growth and migmatite formation

The timing of garnet growth is crucial to interpretation of the thermobarometric data. Due to the high-grade, granoblastic nature of the rocks, timing of garnet growth with respect to fabric development is not always clear in the field or thin section. The garnets sometimes have weakly developed pressure shadows of biotite and plagioclase, which indicates that the garnets grew before or during the final phase of deformation. Inclusions in garnet include quartz, K-feldspar, and fibrolitic sillimanite and are consistent with the matrix assemblage. Monazite inclusions in garnet range in age from 1665 ± 12 to 1746 ± 6 Ma with no spatial relations noted, consistent with garnet growth during (or after) 1.67 Ga. Based on the complex metamorphic history of these rocks, it seems likely that garnet growth occurred more than once. However, EMPA analysis of these garnets reveals that they are largely unzoned (Appendix 4). Similarly, EMPA analyses show that garnet, biotite, K-feldspar and plagioclase in the matrix are chemically homogeneous and unzoned, and that biotite inclusions in garnet are the same as biotite in the matrix (Appendix 4). This suggests that the final metamorphic event to affect these rocks had elevated temperatures for a prolonged period of time such that all major phases were in equilibrium. This is reflected by the values of ~740 °C given by garnet–biotite thermometry (Fig. 13). Therefore, we conclude that the dominant foliation and migmatitic layering in these rocks formed at peak metamorphic conditions of 3.5–5 kb and ~740 °C at 1.67 Ga.

In the McCullough Mountains immediately to the east of the Ivanpah Mountains (Fig. 2), Thomas et al. (1988) estimated the *P–T* conditions of garnet–sillimanite–cordierite-bearing gneisses as 600–775 °C and 2.2–3.6 kb. Young et al. (1989) documented systematic variation in the Fe/Mg ratio in cordierite grains as inclusions in garnet and in the matrix. They interpreted the cordierite growth as a continuous reaction during isothermal decompression from ~6 to ~3 kb and at ~750 °C. Although the cordierite in the Ivanpah Mountains is unzoned with respect to Fe/Mg, garnet–biotite and GASP thermobarometry indicates that peak metamorphism occurred at ~3.5 kb and ~740 °C which agrees with the *PT* estimates from the McCullough Mountains (Thomas et al., 1988) and the Cerbat Mountains (Duebendorfer et al., 2001). This suggests that the 1.67 Ga high-grade metamorphic event may have been widespread.

From 1.68 to 1.66 Ga, numerous continentally derived plutons were emplaced in several locations across the Mojave province, including batholith-sized granitic plutons in the New York Mountains to the east of the Ivanpah Mountains (Wooden and Miller, 1990; Hawkins et al., 1996; Barth et al., 2009). Therefore, the 1.67 Ga event recorded in the Ivanpah Mountains may have been associated with widespread, regional magmatism, and the low pressure granulite facies conditions could indicate continental extension.

9.3. Regional implications

The Proterozoic rocks of the Ivanpah Mountains preserve a ~100 million years of tectonic and metamorphic events during a major period of continental growth along a convergent margin that migrated to the east through time (Fig. 1). The oldest rocks in the Ivanpah Mountains are paragneisses that contain a distinctive detrital zircon age population with analyses in two age groups: 1.8–2.0 and 2.5–2.7 Ga (Fig. 7). Deposition was followed by rapid burial and the intrusion of the 1.76 Ga gabbro, tonalite and augen granite igneous suite. In the San Bernardino Mountains of southeastern California, a nearly identical suite of rocks has been described and interpreted as an island arc system that formed on or adjacent to pre-existing continental crust (Barth et al., 2000).

The source of the Proterozoic metasediments in the Mojave province is unknown. A North American source is likely; crust of the Trans-Hudson orogenic belt could be the source of ~1.8–2.1 Ga zircons, and Late Archean zircon ages are common to the Wyoming province (e.g. Chamberlain et al., 2003). In addition, the whole rock geochemistry indicates a deposition proximal to a continental source (Wooden and Miller, 1990). Therefore we propose that the Mojave province was formed near the North American margin, possibly in a back arc setting, and was quickly accreted after its formation. However, Shufeldt et al. (2010) determined that the Vishnu schist of the Grand Canyon had zircons that were more like the Australia (Gawler) craton than Wyoming.

The timing of regional deformations preserved in the Ivanpah Mountains has implications for the nature of tectonic assembly of the Mojave province with the adjacent Yavapai province and North America. Duebendorfer et al. (2001) also reported two periods of deformation and metamorphism in the Cerbat Mountains of the eastern Mojave: an early period of migmitization at 5–6 kb and 675 to ~740 °C that is bracketed between 1.74 and 1.72 Ga, followed by isothermal decompression and a second metamorphic event at 3.5–4.5 kb and 650–700 °C which occurred between 1.72 and 1.68 Ga. They proposed that the Mojave and Yavapai terrains collided first at ca. 1.74–1.72 Ga, and that the combined tectonic block collided with North America during the ca. 1.70 Ga Ivanpah orogeny. This was followed by continental stabilization and the intrusion of numerous crustally derived plutons at 1.68 Ga (Duebendorfer et al., 2001). The similarities between the Ivanpah

Mountains and the Cerbat Mountains are striking. However, the ages of initiation of calc-alkaline plutonism attributed to arc magmatism range from 1.79 to 1.76 Ga in the western Mojave province, 1.76–1.74 in the eastern Mojave, and 1.74–1.72 Ga in the Yavapai province (Karlstrom and Bowring, 1988; Barth et al., 2009, this study), and thus we prefer a model of more or less continuous arc formation and accretion onto North America. The presence of 1.74 Ga metamorphism and deformation in both provinces suggests that they were joined at or before that time.

In the Ivanpah Mountains, the record of older accretionary tectonics is largely obliterated by pervasive migmitization that occurred at 1.67 Ga. In the Grand Canyon, rocks of the Mojave Province experienced rapid decompression from 1.690 to 1.676 Ga (Hawkins and Bowring, 1997), indicating that the Mojave province underwent a period of regional extension at ca.1.67 Ga. At this time, rocks of the Mazatzal province were being formed as island arcs along an active margin in central New Mexico, but deformation of these rocks in the Mazatzal orogeny occurred after ca. 1.65 Ga (Karlstrom et al., 2004; Amato et al., 2008). Therefore it seems more likely that the low pressure granulite facies metamorphism preserved in the Ivanpah Mountains was related to the collapse of over-thickened crust (i.e. metamorphic core complex). More detailed studies of the rocks exposed in the Mojave province are required to test this theory.

10. Conclusions

Banded gneisses from the Ivanpah Mountains record over 100 million years of tectonic events that occurred during the Paleoproterozoic. The oldest rocks are paragneisses made up of immature metasediments that were deposited ca. 1.79–1.76 Ga, and intruded by gabbro, tonalite, and granite at 1.76 Ga. These units likely formed in an arc setting on or adjacent to a continent. Metamorphism, deformation and partial melting occurred initially at 1.74 Ga. Evidence for metamorphism during the 1.70 Ga Ivanpah orogeny, as defined by Wooden and Miller (1990), is present in metamorphic zircon, but no monazites or igneous rocks of that age have been found. The final phase of metamorphism, deformation and intrusion of leucocratic dikes occurred at 1.67 Ga. Growth of metamorphic minerals, including garnet, cordierite, sillimanite, and K-feldspar occurred at this time. Peak metamorphic conditions from this phase of growth were ~740 °C and 3–4 kb although cordierite growth was late and at a lower pressure. We propose that the migmatites exposed in the Ivanpah Mountains represent a period of extension, partial melting, and magmatism at 1.67 Ga not previously identified in the Mojave province.

Acknowledgments

We would like to acknowledge several people who made this research possible. We thank Elizabeth Miller for her support, revisions and numerous discussions of this manuscript. We also thank Andy Barth for helpful discussions. Mike Spicuzza aided in the generation of the laser fluorination data, and John Fournelle assisted with the electron microprobe data. We than Brad Ito for his assistance with the SHRIMP-RG, and Noriko Kita and Jim Kern for their assistance on the IMS-1280. We also thank Brian Hess for help with sample preparation. Wisc-SIMS is funded by the National Science Foundation (EAR-0319230, 0744079, and 1053466).

Appendix A. Analytical techniques

All samples were prepared for SIMS analysis at the Stanford University mineral separations facility by use of standard crushing and density separation techniques. Samples were passed through a Frantz magnetic separator and then hand picked under a binocular microscope. Grains were cast in epoxy, polished and imaged by back scattered electrons (BSE) or cathodoluminescence (CL) prior to analyses. The identification of micro-mineral inclusions was done in thin section using energy dispersive X-ray analysis (EDS).

U–Th–Pb analyses of zircon and monazite were conducted on the SHRIMP-RG (reverse geometry) ion microprobe co-operated by U.S. Geological Survey and Stanford University in the SUMAC facility at Stanford University. Minerals, concentrated by standard heavy mineral separation processes and hand picked for final purity were mounted on double stick tape on glass slides in 1×6 mm rows, cast in epoxy, ground and polished to a 1 μm finish on a 25 mm diameter by 4 mm thick disc. All grains were imaged with transmitted light and reflected light (and incident light if needed) on a petrographic microscope, and with cathodoluminescence (zircons) and back scattered electrons (monazite) on a JEOL 5600 SEM to identify internal structure, inclusions and physical defects. The mounted grains were washed with EDTA solution and distilled water, dried in a vacuum oven, and coated with Au. Mounts typically sit in a loading chamber at high pressure (10–7 torr) for several hours before being moved into the source chamber of the SHRIMP-RG. Secondary ions were generated from the target spot with an O_2^- primary ion beam varying from 2 to 6 nA. The primary ion beam typically produces a spot with a diameter of 20–40 μm and a depth of 1–2 μm for an analysis time of 9–12 min. Smaller spot diameters (<20 μm) and smaller primary beam currents (<2 nA) were used if U or Th concentrations were very high (i.e. monazites) or internal structures were very fine. Nine peaks were measured sequentially for zircons (the SHRIMP-RG is limited to a single collector, usually an EDP electron multiplier): $^{90}Zr_2{}^{16}O$, ^{204}Pb, Background (0.050 mass units above ^{204}Pb), ^{206}Pb, ^{207}Pb, ^{208}Pb, ^{238}U, $^{248}Th^{16}O$, $^{254}U^{16}O$. Autocentering on selected peaks and guide peaks for low or variable abundance peaks (i.e. $^{96}Zr^{216}O$ 0.165 mass unit below ^{204}Pb) were used to improve the reliability of locating peak centers. The number of scans through the mass sequence and counting times on each peak were varied according to sample age and U and Th concentrations to improve counting statistics and age precision. Measurements were made at mass resolutions of 6000–8000 (10% peak height). The SHRIMP-RG was designed to provide higher mass resolution than the standard forward geometry of the SHRIMP I and II (Clement and Compston, 1994). This design also provides very clean backgrounds and combined with the high mass resolution, the acid washing of the mount, and rastering the primary beam for 90–120 s over the area to analyzed before data is collected, assures that any counts found at mass of ^{204}Pb were actually Pb from the zircon and not surface contamination. In practice greater than 95% of the spots analyzed have no common Pb. Concentration data for zircons were standardized against zircon standard VP-10 (1200 Ma, granitoid, Joshua Tree National Park, CA; Bath and Wooden, unpublished) which was analyzed repeatedly throughout the duration of the analytical session. Data reduction follows the methods described by Williams (1997) and Ireland and Williams (2003) and uses the Squid and Isoplot programs of Ken Ludwig.

For monazite analyses, excess ^{204}Pb counts had been noted in the USGS-Stanford lab since 1999. These counts were attributed to a double charged molecule, $Th^{144}NdO$, that had the same mass as ^{204}Pb. A correction was developed for this excess ^{204}Pb by measuring $^{232}Th^{143}NdO$ which occurs at the half mass position (203.5) and subtracting a proportional number of counts from those measured at mass ^{204}Pb. Particularly for Phanerozoic monazite analyses, this correction brought analyses from slightly below a Terra-Wasserburg concordia to being within error of concordia. This same correction was used routinely for Precambrian monazites. Ages for suite of Precambrian monazites analyzed by TIMS were reproduced using this correction method on ion microprobe data from the SHRIMP-RG. However, doing the course of this study

it was noted that monazites with U concentrations below 500 ppm gave common Pb corrected ages that appeared to be too low while their uncorrected ages gave ages similar to samples with higher U concentrations. Analytical work at the Research School of Earth Sciences, Australian National University, had success using energy filtering on a SHRIMP II to remove molecular interferences in monazite analyses. Energy filtering is somewhat different on the SHRIMP-RG as a result of the differences in geometry of the two instruments. An experiment utilizing energy filtering on the SHRIMP-RG was conducted using reference monazites with TIMS ages and a mix of Phanerozoic and Precambrian monazites run previously on the SHRIMP-RG. The intensity of the ThO beam was reduced to 1/3 of its unfiltered value. For most monazites this eliminated counts at ^{204}Pb. When counts were present, a normal common Pb correction was applied. Results for Tertiary and Mesozoic monazites were essentially the same by both methods. Precambrian monazites with U concentrations above 1000 ppm also gave equivalent results by both methods. However, monazites with lower U concentrations gave higher ^{207}Pb/^{206}Pb ages with energy filtering than those that resulted from the ThNdO correction. In all cases the ^{207}Pb/^{206}Pb ages from energy filtering were equivalent within error to the uncorrected ages from analyses without energy filtering. However, energy filtering does seem to minimize the occurrence of analyses that plot above concordia (reverse discordance) suggesting that likely matrix issues are also reduced by energy filtering. Therefore, we are using the ages calculated from uncorrected data in this paper.

Oxygen isotope analysis was performed at the University of Wisconsin WiscSIMS laboratory using a CAMECA IMS-1280 ion microprobe following the procedures outlined in Kita et al. (2009) and Valley and Kita (2009). The zircon mounts were top mounted with the KIM-5 oxygen isotope standard (Valley, 2003, δ^{18}O = 5.09‰ VSMOW), and re-polished prior to oxygen isotope analyses. Extra care was taken to achieve a smooth, flat, lower relief polish. A focused Cs+ primary beam was used for analysis at 1.9–2.2 nA and a corresponding spot size of 10–12 μm. A normal incident electron gun was used for charge compensation. The secondary ion acceleration voltage was set at 10 kV and the oxygen isotopes were collected in two Faraday cups simultaneously. Data were acquired over four separate sessions. Four consecutive measurements of zircon standard KIM-5 were analyzed at the beginning and end of each session, and every 10–20 unknowns throughout each session. The average values of the standard analyses that bracket each set of unknowns were used to correct for instrumental bias. The average precision (reproducibility) of the bracketing standards for this study ranged from ±0.07 to ±0.50 and averaged ±0.27‰ (2SD). After oxygen isotope analysis, ion microprobe pits were imaged by secondary electron microscopy and pits that were located on obvious cracks or inclusions were excluded from the data set.

Appendix B. Supplementary data

Supplementary data associated with this article can be found, in the online version, at http://dx.doi.org/10.1016/j.precamres.2012.09.006.

References

Amato, J.M., Boullion, A.O., Serna, A.M., Sanders, A.E., Farmer, G.L., Gehrels, G.E., Wooden, J.L., 2008. The evolution of the Mazatzal province and the timing of the Mazatzal orogeny: insights from U-Pb geochronology and geochemistry of igneous and metasedimentary rocks in southern New Mexico. Geological Society of America Bulletin 120, 328–346.

Armstrong, J.T., 1995. CITZAF: a package of correction programs for the quantitative electron microbeam X-ray analysis of thick polished materials, thin films and particles. Microbeam Analysis 4, 177–200.

Barth, A.P., Wooden, J.L., Coleman, D.S., Fanning, C.M., 2000. Geochronology of the proterozoic basement of southwesternmost North America, and the origin and evolution of the Mojave crustal province. Tectonics 19 (4), 616–629.

Barth, A.P., Wooden, J.L., Coleman, D.S., Vogel, M.B., 2009. Assembling and disassembling California: a zircon and monazite geochronologic framework for Proterozoic crustal evolution in southern California. Journal of Geology 117, 221–239.

Bennett, V.C., DePaolo, D.J., 1987. Proterozoic crustal history of the western United States as determined by Neodymium isotopic mapping. Geological Society of America Bulletin 99, 674–685.

Bowman, J.R., Moser, D.E., Valley, J.W., Wooden, J.L., Kita, N.T., Mazdab, F.K., 2011. Zircon U-Pb isotope, δ^{18}O and trace element response to 80 m.y of high temperature metamorphism in the lower crust: sluggish diffusion and new records of Archean craton formation. American Journal of Science 311, 719–772.

Bryant, B., Wooden, J.L., Nealey, L.D., 2001. Geology, geochronology, geochemistry, and Pb-isotopic compositions of Proterozoic rocks, Poachie region, west-central Arizona – a study of the east boundary of the Proterozoic Mojave Crustal Province. United States Geological Survey Professional Paper 1639, 54 pp.

Chamberlain, K.R., Frost, C.D., Frost, R.B., 2003. Early Archean to Mesoproterozoic evolution of the Wyoming Province; Archean origins to modern lithospheric architecture. Canadian Journal of Earth Sciences 40, 1357–1374.

Clement, S.W.J., Compston, W., 1994. Ion Probe Parameters for Very High Resolution without Loss of Sensitivity, vol. 1107. U. S. Geological Survey Circular, 62 p.

Condie, K.C., 1982. Plate-tectonics model for Proterozoic continental accretion in the southwestern United States. Geology 10, 37–42.

DeWitt, E.d., Kwak, L.M., Zartman, R.E., 1987. U-Th-Pb and ^{40}Ar/^{39}Ar dating of the Mountain Pass carbonatite and alkalic igneous rocks, S.E. California. Geological Society of America Abstracts with Programs 19, 642.

Donovan, J.D., Kremser, D., Fournelle, J., 2010. User's Guide and Reference – Enterprise Edition. Probe Software, Eugene.

Duebendorfer, E.M., Chamberlain, K.R., Jones, C.S., 2001. Paleoproterozoic tectonic history of the Cerbat Mountains, northwestern Arizona: implications for crustal assembly in the southwestern United States. Geological Society of America Bulletin 113, 575–590.

Duebendorfer, E.M., Chamberlain, K.R., Fry, B., 2006. Mojave-Yavapai boundary zone, southwestern United States: a rifting model for the formation of an isotopically mixed crustal zone boundary. Geology 34, 681–684.

Duebendorfer, E., Bonamici, C.E., Portis, D., Prante, M., 2010. Refoning the early history of the Mojave-Yavapai collision: pre-collision rifting and post-collision gravitational collapse. Geological Society of America Abstracts with Programs 42, 413.

Hawkins, D.P., Bowring, S.A., Ilg, B.R., Karlstrom, K.E., Williams, M.L., 1996. U-Pb geochronologic constraints on Proterozoic crustal evolution: Geological Society of America Bulletin 108, 1167–1181.

Hawkins, D.P., Bowring, S.A., 1997. U-Pb systematics of monazite and xenotime: case studies from the Paleoproterozoic of the Grand Canyon, Arizona. Contributions to Mineralalogy and petrology 127, 87–103.

Hodges, K.V., Spear, F.S., 1982. Geothermometry, geobarometry and the Al_2SiO_5 triple point at Mt. Moosilauke, New Hampshire. American Mineralogist 67, 1118–1134.

Hoffman, P.F., 1988. United plates of America, the birth of a craton: early Proterozoic assembly and growth of Laurentia. Annual Review of Earth and Planetary Sciences 16, 543–603.

Ilg, B.R., Karlstrom, K.E., Williams, M.L., 1996. Tectonic evolution of Paleoproterozoic rocks in the Grand Canyon – insights into middle-crustal processes. Geological Society of America Bulletin 108 (9), 1149–1166.

Ireland, T.R., Williams, I.S., 2003. Considerations in zircon geochronology by SIMS. In: Hanchar, J.M., Hoskins, W.O. (Eds.), Zircon. Mineralogical Society of America, pp. 215–241.

Karlstrom, K.E., Bowring, S.A., 1988. Early Proterozoic assembly of tectonostratigraphic terranes in southwestern North America. Journal of Geology 96, 561–576.

Karlstrom, K.E., Ahall, K.-I., Harlan, S.S., Williams, M.L., McLelland, J., Geissman, J.W., 2001. Long-lived (1.8–1.0 Ga) convergent orogen in southern Laurentia, its extensions to Australia and Baltica and implications for refining Rodinia. Precambrian Research 111, 5–30.

Karlstrom, K.E., Humphreys, E.D., 1998. Persistent influence of Proterozoic accretionary boundaries in the tectonic evolution of nouthwestern North America: interaction of cratonic grain and mantle modification events. Rocky Mountain Geology 33, 161–179.

Karlstrom, K.E., Amato, J.M., Williams, M.L., Heizler, M., Shaw, C., Read, A., Bauer, J., 2004. Proterozoic tectonic evolution of the New Mexico region: a synthesis. In: Mack, G.H., Giles, K.A. (Eds.), The Geology of New Mexico: A Geologic History. New Mexico Geological Society Special Publication 11. , pp. 1–34.

Karlstrom, K.E., Williams, M.L., 1995. The case for simultaneous deformation, metamorphism, and plutonism: an example from Proterozoic rocks in central Arizona. Journal of Structural Geology 17, 59–81.

Kita, N.T., Ushikubo, T., Fu, B., Valley, J.W., 2009. High precision SIMS oxygen isotope analyses and the effect of sample topography. Chemical Geology 264, 43–57.

Kohn, M., Spear, F., 2003. Program Thermobarometry.

Kohn, M.J., Malloy, M.A., 2004. Formation of monazite via prograde metamorphic reactions among common silicates: implications for age determinations. Geochimica et Cosmochimica Acta 68, 101–113.

Miller, D.M., Wooden, J.L., 1994. Field guide to Proterozoic geology of the New York, Ivanpah, and Providence Mountains, California, U.S. Geological Survey Open-File Report 94–674, 40 p.

Nichols, G.T., Berry, R.F., Green, D.H., 1992. Internally consistent gahnitic spinel-cordierite-garnet equilibria in the FMASHZn system: geothermobarometry and applications. Contributions to Mineralogy and Petrology 111, 362–377.

Page, F.Z., Ushikubo, T., Kita, N.T., Riciputi, L.R., Valley, J.W., 2007. High precision oxygen isotope analysis of picogram samples reveals 2‰ gradients and slow diffusion in zircon. American Mineralogist 92, 1772–1775.

Peck, W.H., Valley, J.W., Graham, C.M., 2003. Slow oxygen diffusion rates in igneous zircons from metamorphic rocks. American Mineralogist 88, 1003–1014.

Pyle, J.M., Spear, F.S., 2003. Four generations of accessory phase growth in low-pressure migmatites from SW New Hampshire. American Mineralogist 88, 338–351.

Seydoux-Guillaume, A.M., Paquette, J.L., Wiedenbeck, M., Montel, J.M., Heinrich, W., 2002. Experimental resetting of the U-Th-Pb system in monazite. Chemical Geology 191, 165–181.

Shufeldt, O.P., Karlstrom, K.E., Gehrels, G.E., Howard, K.E., 2010. Archean detrital zircons in the Proterozoic Vishnu Schist of the Grand Canyon, Arizona: implications for crustal architecture and Nuna supercontinent recontructions. Geology 38, 1099–1102.

Strickland, A., Wooden, J.L., Mattinson, C.G., Miller, D.M., 2009. 130 million years of Paleoproterozoic history recorded by U-Pb monazite and zircon ages form the Ivanpah Mountains, eastern California. Geological Society of America Abstracts with Programs 41, 271.

Thomas, W.M., Clark, H.S., Young, E.D., Orrell, S.E., Anderson, L.J., 1988. Proterozoic high-grade metamorphism in the Colorado River region, Nevada, Arizona, and California. In: Ernst, W.G. (Ed.), Metamorphism and Crustal Evolution of the Western Conterminous United States 526-537. Prentic-Hall, Englewood Cliffs, pp. 526–537.

Valley, J.W., 2003. Oxygen isotopes in zircon. In: Hanchar, J.M., Hoskin, P.W.O. (Eds.), Zircon, 53. Mineralogical Society of America, pp. 343–385.

Valley, J.W., Lackey, J.S., Cavosie, A.J., Clechenko, C.C., Spicuzza, M.J., Basei, M.A.S., Bindeman, I.N., Ferreira, V.P., Sial, A.N., King, E.M., Peck, W.H., Sinha, A.K., Wei, C.S., 2005. 4.4 billion years of crustal maturation: oxygen isotopes in magmatic zircon. Contributions to Mineralogy and Petrology 150, 561–580.

Valley, J.W., Kita, N.T., 2009. In situ oxygen isotope geochemistry by ion microprobe. In: Fayek, M. (Ed.), MAC Short Course: Secondary Ion Mass Spectrometry in the Earth Sciences, 41, pp. 19–63.

Valley, J.W., Chiarenzelli, J.R., McLelland, J.M., 1994. Oxygen isotope geochemistry of zircon. Earth and Planetary Science Letters 126, 187–206.

Whitmeyer, S.J., Karlstrom, K.E., 2007. Tectonic model for the Proterozoic growth of North America. Geosphere 3, 220–259.

Williams, I.S., 1997. U-Th-Pb geochronology by ion microprobe: not just ages but histories. Society for Economic Geologists 7, 1–35.

Wooden, J.L., Miller, D.M., 1990. Chronologic and isotopic framework for Early Proterozoic crustal evolution in the Eastern Mojave Desert Region, SE California. Journal of Geophysical Research 95 (20), 120–133, 146.

Wooden, J.L., DeWitt, E., 1991. Isotopic evidence for the boundary between the Early Proterozoic Mojave and central Arizona crustal provinces in western Arizona. In: Karlstrom, K.E. (Ed.), Proterozoic Geology and Ore Deposits of Arizona. Arizona Geological Society Digest 19, pp. 27–50.

Young, E.D., 1989. Petrology of biotite-cordierite-garnet gneiss of the McCullough Range, Nevada. II. P–T – a path and growth of cordierite during late stages of low P granulite grade metamorphism. Journal of Petrology 30, 61–78.